HIGHWAY RESEARCH RECORD

Number 121

Pavement Design and Evaluation

3 Reports

Presented at the
44th ANNUAL MEETING
January 11-15, 1965

SUBJECT CLASSIFICATION
25 Pavement Design
26 Pavement Performance

HIGHWAY RESEARCH BOARD

of the

Division of Engineering and Industrial Research
National Academy of Sciences—National Research Council
Washington, D. C.

1966

Department of Design

W. B. Drake, Chairman
Assistant State Highway Engineer
Kentucky Department of Highways, Lexington

HIGHWAY RESEARCH BOARD STAFF
F. N. Wray, Engineer of Design
R. C. Edgerton, Assistant Engineer of Design

PAVEMENT DIVISION

Milton E. Harr, Chairman
Professor of Soil Mechanics, School of Civil Engineering
Purdue University, Lafayette, Indiana

COMMITTEE ON PAVEMENT CONDITION EVALUATION
(As of December 31, 1964)

Malcolm D. Graham, Chairman
Director, Bureau of Physical Research
New York State Department of Public Works, Albany

Robert F. Baker, Director, Office of Research and Development, U.S. Bureau of Public Roads, Washington, D.C.
Frederick E. Behn, Assistant Engineer of Specifications and Development, Ohio Department of Highways, Columbus
A. Y. Casanova, III, Acting Chief, Pavement Evaluation Research Branch, Structural Research Division, U.S. Bureau of Public Roads, Washington, D.C.
W. B. Drake, Assistant State Highway Engineer, Kentucky Department of Highways, Lexington
Karl Dunn, Research Engineer, Wisconsin State Highway Commission, Madison
Leroy D. Graves, Associate Professor of Civil Engineering, Notre Dame University, Notre Dame, Indiana
W. S. Housel, University of Michigan, Ann Arbor
W. Ronald Hudson, Department of Civil Engineering, University of Texas, Austin
Louis C. Lundstrom, Director, General Motors Proving Grounds, General Motors Corporation, Milford, Michigan
Alfred W. Maner, Staff Engineer, The Asphalt Institute, University of Maryland, College Park
Phillip L. Melville, Civil Engineering Branch, Engineering Division, Military Construction, Office, Chief of Engineers, Department of the Army, Washington, D.C.
A. B. Moe, Manager, Maintenance Branch, Bureau of Yards and Docks, U.S. Navy, Washington, D.C.
Frank P. Nichols, Jr., Highway Research Engineer, Virginia Department of Highways, Charlottesville
Bayard E. Quinn, Mechanical Engineering School, Purdue University, Lafayette, Indiana
Foster A. Smiley, Maintenance Engineer, Iowa State Highway Commission, Ames
Bertram D. Tallamy, Consulting Engineer, Washington, D.C.
W. E. Teske, Paving Engineer, Portland Cement Association, Chicago, Illinois
Frank Y. Wilkinson, Federal Aviation Agency, Washington, D.C.
Eldon J. Yoder, Joint Highway Research Project, Purdue University, Lafayette, Indiana

Foreword

The three research papers in this Record, although very dissimilar in scope and technical composition, all relate to the general problem of providing satisfactory pavements.

The first paper, by Dr. B. G. Hutchinson on "Conceptual Framework for Pavement Design Decisions," is unique. It presents the fundamentals and suggests the possible application of statistical decision theory to the problems of identifying and evaluating a group of complexly related design elements. The framework of concepts, unlike some definite single theory, is offered as a procedure which allows systematic comparisons of various design solutions.

A new technique for measuring and describing longitudinal profiles for highway pavements has been developed and reported by B. E. Quinn and J. L. Zable at Purdue University. Their paper describes a pavement-elevation power-spectrum method for determining pavement roughness. It refers to an earlier paper by Dr. Quinn who, a few years ago, introduced power spectrum analysis as a meaningful measure of pavement roughness. The principal innovation in the present paper is that data on dynamic tire forces which were taken as a criterion of vehicle performance were utilized in computing elevation power spectra.

The third paper describes the development and use of the new GMR Road Profilometer. Continued interest in such a device by highway engineers engaged in design, construction and maintenance of smooth pavements encouraged the General Motors Corporation research engineers to further develop and simplify this special device, which was already becoming known as a valuable experimental pavement-roughness measuring machine. Fully discussed in this paper is the basic operating principal of the GMR Profilometer, the description of a unit that has been supplied to the Michigan State Highway Department and a presentation of some typical test results.

Contents

A Conceptual Framework for Pavement Design Decisions

B. G. HUTCHINSON, Department of Civil Engineering, University of Waterloo, Waterloo, Ontario

•THE COMPLEX properties and behavior of highway pavement structures have resulted in the evolution of standard pavement design procedures and specifications to aid individual designers in the solution of specific problems. These standard procedures are intended to provide the basic information necessary for the solution of groups of pavement design problems having certain features in common.

The characteristic common to virtually all pavement design decisions is the uncertainty under which they are made. Uncertainty enters into pavement design decisions whenever the outcome of a particular pavement design cannot be exactly predicted. In order to simplify pavement design decisions, it has been expedient, both in actual design decisions and in analytical and empirical models of pavement behavior, to act as if the consequences of various actions could be predicted with certainty.

To overcome this uncertainty, existing pavement design procedures have relied heavily on engineering experience and judgment, much of which is of a subjective nature. This subjectivity has resulted in pavement design procedures whose underlying structure is not always clear, and which cannot easily be modified in the light of new data. Thus, an undesirable situation exists with all standard design procedures where solutions to specific design problems are based more on the forms that have been found as solutions to old problems, rather than on the particular nature of the design problem at hand. Existing pavement design methods do not allow a systematic and objective comparison of various pavement design types, and consequently pavement design decisions are biased by the personal experiences of the designer.

In addition to the uncertainty of future pavement performance, pavement design decisions are essentially economic decisions, and present pavement design procedures do not formally incorporate the economic properties of the various design alternatives. With present methods, economic considerations are implicitly expressed in the various design criteria. However, there has been a tendency to transform these criteria into rigid engineering standards that soon lose all contact with the original economic realities which entered into their development.

It is the purpose of this paper to establish the elements necessary for a rational and conceptually complete pavement design system. In particular, a formal approach to the uncertainty of future pavement performance will be developed, as well as an objective technique for incorporating the economic characteristics of pavement designs.

PAVEMENT DESIGN SYSTEM

A rational pavement design procedure, in which both the technical and economic characteristics of designs as well as the uncertainty of their future performance are objectively accounted for, should contain each of the steps defined below.

Design System Aims

The aim of the pavement design system is to select a pavement design strategy from among alternate designs whose expected present worth is a minimum with respect to the alternate designs, and whose expected life is equal to the design life.

Paper sponsored by Pavement Division of Department of Design.

This definition implicitly assumes that a pavement of adequate serviceability qualities is provided throughout the design life, and that failure occurs when a limiting value of serviceability is attained. Studies by the Bureau of Public Roads (1), Saskatchewan Highway Department (2), Canadian Good Roads Association (3) and others have shown that the age at failure of highway pavements cannot be exactly predicted. Instead, a distribution of the age at failure of highway pavements has been observed for similar pavement designs. Available data suggest that the relative-frequency histograms may be approximated by a normal distribution function. This variability in the age at which failure occurs results from the heterogeneity of materials, variability in climatic conditions and loading, imperfections in the ability of analytical techniques to predict future performance, and so on.

The primary variable associated with the analysis of pavement designs is the age at which failure occurs, A. In view of the above comments, A must be considered as a random variable, $\tilde{A}$. The essential problem in pavement design is to predict the distribution function F(A), or the probability density function f(A) of the random variable, $\tilde{A}$, for each pavement design. In this investigation, random variables are shown as $\tilde{A}$, $\tilde{\theta}$, etc., using the tilde to distinguish the random variable from a particular value of the variable. Also, in taking expectations of random variables, the probability measure with respect to which the expectation is taken is indicated by naming the random variable and the conditions in parentheses following the operator, e.g., $E(\tilde{\theta}|z)$, $E(\tilde{A})$, etc.

Value Parameter

The value parameter expresses the value of each possible outcome of every design strategy to the designer. It is expressed as the present worth in dollar units of each possible outcome.

The present worth of each outcome includes the initial capital costs, annual maintenance costs, and any additional costs associated with pavement failure. The present worth of each outcome may be calculated from

$$PW = \left\{ C \cdot \frac{i(1+i)^A}{(1+i)^A - 1} + AMC \right\} \frac{(1+i)^L - 1}{i(1+i)^L} \tag{1}$$

in which

PW = present worth of outcome,
C = initial capital cost,
i = interest rate,
A = age at failure in years,
AMC = annual maintenance cost, and
L = design life in years.

Since A is a random variable, PW is a random variable. The value associated with a particular design strategy may be expressed as an expected present worth, $E[\tilde{PW}]$. In addition, since $\tilde{PW}$ is a nonlinear function of $\tilde{A}$, $E[\tilde{PW}]$ is dependent on both the mean and standard deviation of the distribution of $\tilde{PW}$.

There are no significant additional costs associated with pavement failure itself, as would be the case with highway bridge failures, where injury and loss of life must be incorporated in the measure of value.

Decision Criterion

The decision criterion is a rule which specifies how value parameters should be combined to obtain a single index of value for assessing the optimality of designs. With the pavement design system, the decision criterion is simply to select that design strategy with the least expected present worth.

Design Constraints

Design constraints are the physical and economic restrictions which may limit the extent of feasible, acceptable or permissible solutions to a design problem.

The only major constraint with the pavement design system is economic, and it is a maximum limit on the expected present worth. This maximum value is dictated by the economic characteristics of the overall highway project, of which the pavement structure is only one element.

Specification of Environmental Conditions

This step involves the quantitative, but in most cases also qualitative, definition or classification of all those environmental factors which influence the performance of alternate design strategies.

This classification not only involves magnitude and number of repetitions of axle loads, but includes all those environmental factors which result in serviceability decrements. The exact nature of this load classification is dependent on the requirements of the analytical or empirical models available for the prediction of probable future behavior of alternate design strategies. It is well known that rigorous analytical and empirical models of pavement behavior are not available, and that available models are imperfect predictors of probable future behavior. It is, therefore, meaningless to attempt to predict precisely the probable distributions of axle loads, climatic conditions, materials properties, etc.

Load definition must be a classificatory procedure which attempts to specify the general environmental conditions which might be expected at each pavement location. Recent studies by the Canadian Good Roads Association reported by Wilkins (4) and others have demonstrated that only a relatively coarse classification of the pavement environment is warranted.

A classificatory approach to probable loadings is also used in structural design formulations, where regions of various environmental conditions are established. Unfortunately, many of these load classification schemes are given numerical connotations completely incompatible with the level of data on which they are based, which are essentially subjective.

Specific environmental classes are not isolated in this paper, since the appropriate number of classes will depend on a particular area. However, the type of classification scheme used by the Canadian Good Roads Association (4) would seem appropriate and sufficiently sensitive.

Design Synthesis

The synthesis of alternate designs involves the development of a set of alternate design strategies which satisfy the design system aims to a greater or lesser degree. Present efforts at innovative design are virtually nonexistent in the design of highway pavements. The unfortunate situation exists where standard designs, or slight modifications of these designs, are used as design solutions. This situation results directly from the fact that no framework has existed within which new design strategies could be evaluated relative to these standard designs. Consequently, few attempts at using new materials and pavement configurations have been forthcoming since those developed some 40 to 50 years ago.

A number of approaches to innovative problem solving have been developed within recent years, but have not been sufficiently well developed to be of immediate practical application.

Design Analysis

This step involves the prediction of the expected age at failure of the set of tentative design strategies, in the light of the physical and economic properties of each design and the environmental conditions.

It has already been established that one of the major requirements of making a rational analysis of pavement design strategies is predicting the distribution of the random variable $\tilde{A}$ associated with each design strategy. In addition, a formal procedure is required to incorporate knowledge gained about the distribution function by prior analysis or experimentation. It has become apparent in recent years (5, 6, 7) that the surface deflection of flexible pavements under a standard 9-kip wheel load is a reliable indicator of future pavement performance. In this paper, it has been assumed for purposes of illustration that a central problem in the analysis of alternate flexible pavement designs is predicting the distribution of the surface deflection f(A) for each design strategy, and then using this distribution to predict the distribution function, F(A). Any reliable indicator of future performance could be used, however, thereby allowing for the direct comparison of flexible, rigid and semirigid pavements.

The information required for this step in the design process is as follows:

1. A listing of all possible design strategies d_1, d_2, d_3, ...
2. The distributions of the age to failure of each of these strategies $f_1(A)$, $f_2(A)$, ...
3. The present worth of each possible outcome of every design strategy PW_1, PW_2, ...
4. Prior information available on the probability distributions mentioned in 2.
5. The possible experiments or analyses that may be performed before selecting a particular design strategy, in order to gain further information about the probability distributions of 2.
6. The cost of these experiments.
7. A listing of the possible outcomes of these experiments.
8. A specification of the reliability of each of these outcomes in predicting the true outcome of a particular design strategy.

The final step of the design process is to use the decision criterion to select the optimum solution to the design problem. In other words, the designer selects that pavement design strategy with the minimum expected present worth. In the next section, the well-developed principles of statistical decision theory are reviewed and used to formulate the design analysis step in a rigorous manner.

STATISTICAL DECISION THEORY

The nature of elementary statistical decision processes is well described by Luce and Raiffa (8), Bross (9) and a number of other writers. Turkstra (10) has advocated the use of these elementary formulations in structural design decisions, while Tribus (11, 12) has also proposed their use in general engineering design and reliability problems. These decision processes are usually expressed in terms of 4 basic parameters:

1. A number of alternate courses of action open to the decision maker;
2. A number of states of nature that may obtain after a particular course of action has been selected;
3. The probability measures defined over the states of nature; and
4. The desirabilities of each of the outcomes that result from combinations of specific courses of action and particular states of nature.

An important extension of these elementary decision processes involves a methodology for taking into account knowledge gained about the states of nature by experimentation or theoretical analysis before selecting a particular course of action. This formulation is much more appropriate with respect to pavement design problems than the elementary formulations mentioned above. A great deal of prior information is available in the form of theoretical and empirical models of behavior which can be used to predict future behavior. These predictions may be imperfect, but the formulation described below allows this imperfection to be formally evaluated.

The basic data required for any decision problem in which experimentation or analysis is feasible prior to the selection of a particular course of action are:

1. A listing of the possible terminal decisions d_1, d_2, ...
2. A listing of the possible states of nature that may occur after a particular course of action has been selected θ_1, θ_2, ...
3. A listing of the possible experiments or analyses that may be performed prior to the selection of a terminal decision e_0, e_1, e_2, ...
4. A listing of the outcomes of these experiments z_0, z_1, z_2, ... which the decision maker believes possible; the likelihoods of these experimental observations depend on what the true state of nature actually is.
5. A listing of the values or utilities which represent the decision maker's preferences for all e, z, a, θ combinations or strategies.
6. A listing of the probabilities which the decision maker assigns to the joint probability distribution of z, θ for each of the potential experiments or methods of analyses.

The problem facing the decision maker is to select a course of action after observing the outcome of a prior experiment. Raiffa and Schlaifer (13) describe 2 basic modes of analysis of a decision problem, and both of these methods of analysis are important in evaluating pavement design decisions. One mode of analysis is concerned with the choice of a terminal action, after an experiment has already been performed and its outcome observed. This method of analysis is known as the terminal or posterior

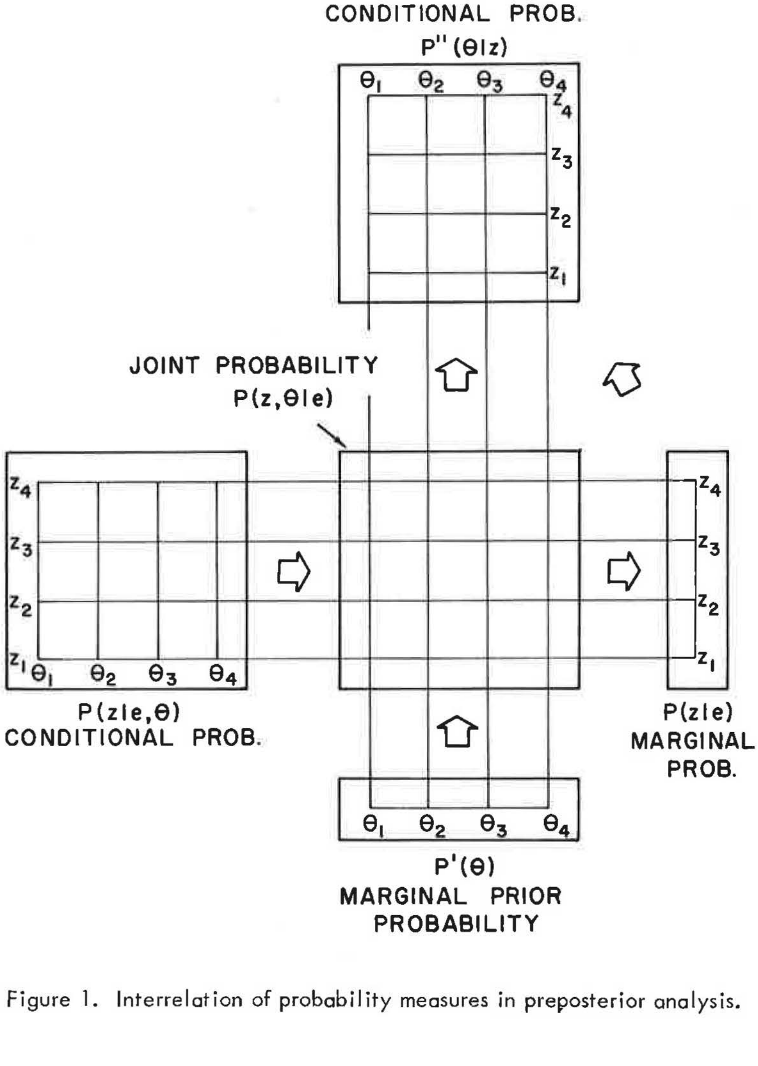

Figure 1. Interrelation of probability measures in preposterior analysis.

analysis. The second method is known as preposterior analysis, and is concerned with the selection of the most valuable experiment to be performed.

Preposterior Analysis

The central problem with respect to both forms of analysis is to assign either directly or indirectly a joint probability measure $P(\theta, z|e)$ to the joint distribution of θ, z for each experiment. In other words, the decision maker must define the reliability of each possible experimental outcome in predicting the true state of nature for each experiment or method of analysis.

The joint probability measures determine 4 other probability measures which are defined below and shown in Figure 1 for a simple case involving a single experiment:

1. The marginal probability measure $P'(\theta)$ on the states of nature that the decision maker would assign to Θ prior to knowing the outcome z of the experiment e.
2. The conditional probability measure $P(z, e|\theta)$ on the space Z of experimental outcomes for a given experiment e, where θ is the true state of nature.
3. The marginal probability measure $P(z|e)$ on the space Z for all θ, and for a specified e.
4. The conditional measure $P''(\theta|z)$ on the state space for a given e and z, which is the probability measure the decision maker assigns to the state space posterior to knowing the outcome z of the experiment e.

The interrelationship of these elements is best shown in the form of a tree diagram of the type shown in Figure 2, which is an abstraction of a simple decision situation in which there is only one possible experiment e_1. Experiment e_0 represents the special case in which no experiment is performed before selecting a course of action.

The manner in which numerical values of the probability measures are arrived at in a particular design problem will be dependent on the particular problem. The most efficient techniques for arriving at probability measures for the pavement design system are discussed later. For the present, it is convenient to assume that the prob-

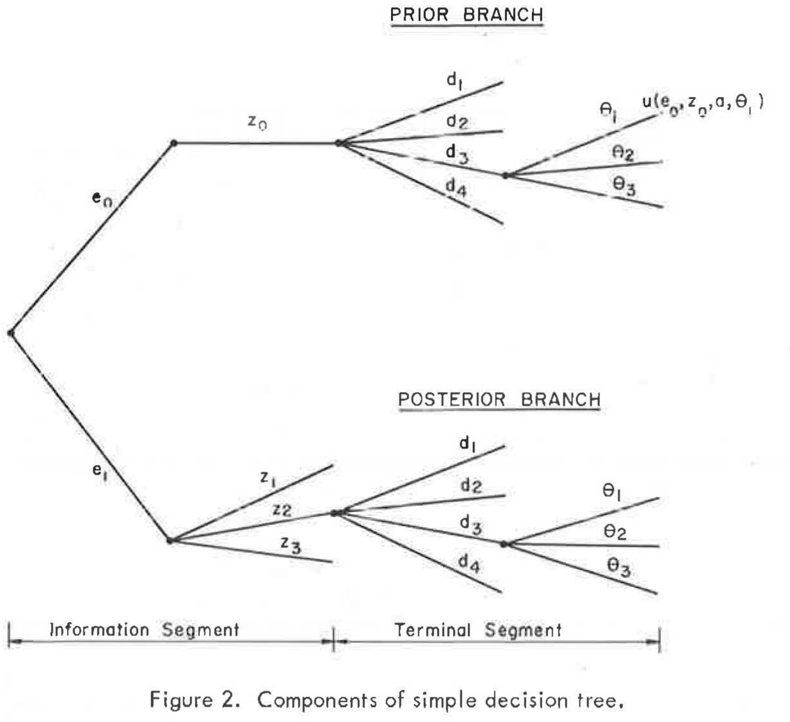

Figure 2. Components of simple decision tree.

ability measures have been defined, and the preposterior form of analysis proceeds by working backwards from the end of the decision tree to the initial point.

It begins by determining the terminal action that should be selected if an experiment has been performed and a particular outcome observed. Since the state of nature is a random variable, only the expected utility associated with each terminal action may be computed

$$u(e, z, d) = E(\tilde{\theta}'' | z) [u(e, z, d, \tilde{\theta})] \tag{2}$$

and the optimal terminal action is given by that action with the maximum expected utility

$$u(e, z) = \max_d u(e, z, d) \tag{3}$$

Similarly the outcome of each experiment is a random variable, and the utility of each experiment can only be computed as an expected utility

$$u(e) = E(z | e) [u(e, \tilde{z})] \tag{4}$$

The experiment with maximum expected utility can be readily selected, and the utility associated with the optimal strategy of the decision problem selected

$$\begin{aligned} u &= \max_e u(e) \\ &= \max_e E(z | e) \left\{ \max_d E(\theta'' | z) [u(e, z, d, \theta)] \right\} \end{aligned} \tag{5}$$

The posterior mode of analysis also has as its ultimate aim the description of an optimal strategy. It arrives at the same strategy as the preposterior form of analysis, but it arrives there by a different technique (13).

Design Example

To illustrate the application of the statistical principles to the previously outlined pavement design process, a simple example involving the evaluation of a new pavement design is given below.

Assume that a standard pavement design for an asphaltic-concrete pavement has evolved in a particular area for certain subgrade soil conditions, traffic loadings, and environment. The expected present worth of providing this standard design is $60,000 per mi for a 20-yr design life. The expected present worth is arrived at by summing the products of the relative frequency of each age to failure and the present worth of providing a pavement assuming that it fails at each of these ages. An alternate pavement design is under consideration for the same conditions of service, and experience in other areas suggests that it could be provided for a present worth of $36,000 per mi for a 20-yr life.

Further, assume that previous experience with this type of pavement in other areas indicates that satisfactory performance has been obtained about 70 percent of the time for similar service conditions. It is possible to obtain additional information about the probable behavior of the pavement type under local conditions by constructing a test section and performing load tests on this section. Previous load testing programs have indicated that if the deflection of the pavement under a standard 9-kip wheel load is less than 0.030 in., satisfactory performance is obtained in about 90 percent of the cases. Deflections greater than 0.030 in. have indicated unsatisfactory performance about 90 percent of the time.

This design problem resolves to one of deciding whether to obtain local information by constructing a test section which will provide more definite information about the probable behavior of pavements constructed with local materials, and then, on the basis of this initial action, whether to accept or reject the tentative design. The design problem is most readily illustrated in tree form of the type shown in Figure 3. The elements of this tree are as follows.

1. Actions:
   d_1—accept new design
   d_2—reject new design
2. States of nature:
   θ_1—satisfactory performance
   θ_2—unsatisfactory performance
3. Experiments:
   e_0—no experiment
   e_1—experiment
4. Experimental outcomes:
   z_0—dummy outcome of e_0
   z_1—deflection <0.030 in. more favorable to θ_1
   z_2—deflection >0.030 in. more favorable to θ_2
5. Utilities
   The utility or value associated with each possible strategy of the decision tree (Fig. 3) may be readily determined from the cost data given above. For example,

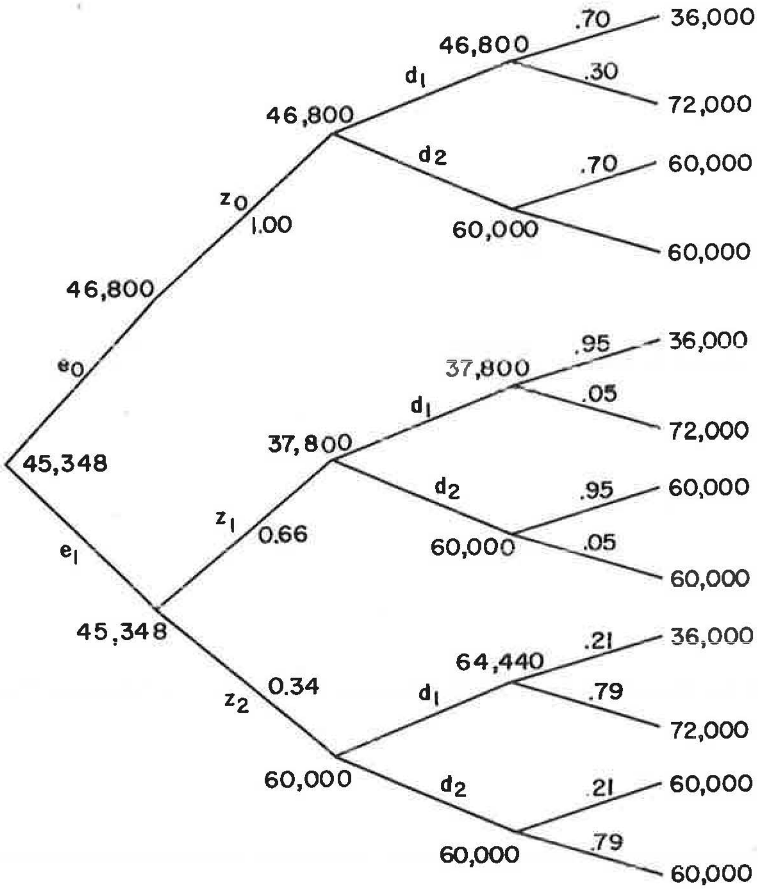

Figure 3. Preposterior analysis of pavement design decision.

if the strategy is selected which involves no experimentation and accepting the new design, the present worth would be $35,000 per mi if it performs satisfactorily, and $72,000 if it is unsatisfactory. The additional $37,000 per mi in the latter case arises from the cost of reconstruction of the failed pavement. If the new design is rejected, then the present worth of providing the standard design is $60,000 per mi. The cost of constructing the test section has not been included in the posterior branch, since this cost is trivial in this particular example. However, it could easily be shown as an additional annual cost.

The immediate problem is to generate probability measures over the joint probability distribution of θ and z. The prior marginal probability measures over the states of nature are

$$P'(\theta_1) = 0.70$$
$$P'(\theta_2) = 0.30$$

The conditional probability measures of obtaining the experimental outcome Z when θ and e exist have also been defined and are given by

$$P(z_1|e_1, \theta_1) = 0.90 \qquad P(z_2|e_1, \theta_1) = 0.10$$
$$P(z_2|e_1, \theta_2) = 0.90 \qquad P(z_1|e_1, \theta_2) = 0.10$$

where the first statement means the probability of obtaining the outcome z_1, when e_1 is the experiment and θ_1 the true state of nature, is 0.90. The joint probability measure on the $\Theta \times Z$ space is given by the product of the prior and conditional measures, since they are independent events

$$P(z_1, \theta_1|e_1) = 0.70 \times 0.90 = 0.63$$
$$P(z_2, \theta_1|e_1) = 0.70 \times 0.10 = 0.07$$

$$P(z_2, \theta_2|e_1) = 0.30 \times 0.90 = 0.27$$
$$P(z_1, \theta_2|e_1) = 0.30 \times 0.10 = 0.03$$

The marginal probability measures of the outcomes z_1 and z_2 of the experiment may be determined by summing over z_1 and z_2, respectively, from the above joint measures

$$P(z_1|e_1) = 0.63 + 0.03 = 0.66$$
$$P(z_2|e_1) = 0.27 + 0.07 = 0.34$$

From Bayes' theorem $P''(\theta|z) = \dfrac{P'(\theta)\ P(z|\theta)}{\Sigma\Theta P(z|\theta)}$ the posterior probabilities over the states of nature are then determined

$$P''(\theta_1|z_1) = 0.63/0.66 = 0.95 \qquad P''(\theta_1|z_2) = 0.21$$
$$P''(\theta_2|z_1) = 0.05 \qquad P''(\theta_2|z_2) = 0.79$$

These posterior probabilities of state represent a revised set of probabilities given an experiment and a particular result of this experiment. The probability measures have been indicated on the appropriate elements of the decision tree (Fig. 3).

The optimum strategy can now be established by calculating the expected annual cost of each possible action, and selecting that action with the least expected annual cost. For example,

$$u(e_0, z_0, d_1) = 0.7 \times 36{,}000 + 0.3 \times 72{,}000 = \$46{,}800$$

and

$$u(e_0, z_0, d_2) = \$60{,}000$$

Therefore the strategy $e_0\ z_0\ d_1$ represents the optimum action of the prior branch. By proceeding in a similar manner with the posterior branch, it can easily be verified that the optimum strategy for the decision situation shown is to construct a test section, and to accept the new pavement design if a deflection less than 0.030 in. is obtained, since this strategy results in the least expected annual cost.

While the design situation examined above may be somewhat trivial, it is typical of many pavement design situations. An actual experiment may not be performed, but experimentation may consist of some form of analysis, in which known materials properties are used along with a theoretical or empirical model. In certain design problems, it is possible that the available historical evidence bears much more directly on the posterior measure $P''(\theta|z)$ and the marginal measure $P(z|e)$, than on the complementary measures $P(z|e, \theta)$ and $P'(\theta)$. Instead of computing the posterior measures, the prior measures are calculated, and the utility or value of carrying out experimentation or analysis may be evaluated, as opposed to using a standard design.

ANALYTICAL FORMULATION

The application of the preposterior analysis to a simple pavement design problem was illustrated above, wherein the required computations were carried out numerically. In the majority of pavement design problems numerical analysis would be extremely tedious because of the relatively large sample and state spaces. Raiffa and Schlaifer (13) have shown that both the preposterior and posterior modes of analysis may be formulated analytically, providing the following conditions are met: (a) the experimental outcome can be described by a sufficient statistic of fixed dimensionality, and (b) the prior probability measure $P'(\theta)$ on Θ is conjugate to the conditional probability measure $P(z|e, \theta)$ on the sample space Z.

It was established that, as a first approximation, the distribution of the age at failure, f(A), and the distribution of the surface deflection, f(Δ), may be considered to be normally distributed. Raiffa and Schlaifer have developed the appropriate distribution theory for a normal data generating process in which the above conditions are valid. The major points of the distribution theory are reviewed briefly, and it is shown how the pavement design system previously formulated may be expressed in terms of these principles.

Sufficient Statistics

The only complete way of describing the outcome of an experiment is to list all the experimental observations in the order in which they have been observed. However, for analytical purposes, the need is to establish whether there exists a set of descriptions which is simpler and easier to manipulate, yet contains all the information relative to the decision problem.

The sufficiency of a statistic depends on the particular functional form selected for a decision problem. For example, the statistics sufficient for the description of experimental outcomes generated by a normal process will differ from those sufficient for the description of a Poisson data-generating process. It can be shown (13) that the number of random variables observed, the mean value of the random variables, and the standard deviation are the statistics sufficient to describe fully a sample generated by a normal process.

Conjugate Distributions

If the prior distribution of the random variable θ has a mass function D', then it follows from Bayes' theorem that the posterior distribution of θ is given by

$$D''(\theta|z) = D'(\theta)\ell(z|\theta)N(z) \tag{6}$$

where

$\ell(z|\theta)$ = the probability, given that θ is the true state of nature, that experiment e results in the outcome z; the value assumed by $\ell(z|\theta)$ is termed the likelihood of obtaining an experimental outcome

and

$N(z)$ = normalizing constant given by

$$N(z) = \Sigma\Theta\, D'(\theta)\ell(z|\theta) \tag{7}$$

For any mass function D of θ, and if K is another function on Θ such that

$$D(\theta) = \frac{K(\theta)}{\Sigma\Theta K(\theta)} \tag{8}$$

then

$$D(\theta) \propto K(\theta) \tag{9}$$

and K is called a kernel of the mass function of θ. Similarly, if the likelihood of z given θ is $\ell(z|\theta)$, and ρ and k are functions on Z such that for all z and θ

$$\ell(z|\theta) = k(z|\theta)\,\rho(z) \tag{10}$$

then $k(z|\theta)$ is called a kernel of the likelihood of z given θ, and $\rho(z)$ is called the residue of this likelihood. That is, the kernel is that portion of the likelihood that depends on the state of nature θ.

It may be shown (13) that, using Eqs. 8 and 9, Eq. 6 may be expanded to give

$$D''(\theta|z) \propto K'(\theta)\,k(z|\theta) \tag{11}$$

If the experimental outcome can be described by a sufficient statistic y, then Raiffa and Schlaifer show that Eq. 11 may be rewritten

$$D''(\theta|y) \propto K'(\theta)\,k(y|\theta) \tag{12}$$

That is, the kernel function k is defined as a function $k(\cdot|\theta)$ with parameter θ on the reduced sample space Y. Instead, it may be considered as a function $k(y|\cdot)$ with parameter y on the state space Θ. This function when normalized and shown to be non-negative for all $\theta \in \Theta$ is called a natural conjugate with parameter y of the kernel function k. That is, the roles of the variables and parameters in the algebraic expression of the sample likelihood function are interchanged.

The mathematical simplification introduced by Raiffa and Schlaifer is to select the functional form of the prior distribution such that its kernel has the same mathematical form as the sample kernel. The 2 kernels are then combined to give a closed expression for the desired posterior probabilities.

Normal Data Generating Process

If the data generating process is normal, Raiffa and Schlaifer show that closed mathematical expressions for the sample, prior, and posterior probability distributions can be derived. It has been pointed out above that the general procedure involves the selection of a prior distribution such that the kernel of the distribution is of the same mathematical form as the sample kernel.

The normal data generating process is defined in the following manner by Raiffa and Schlaifer:

$$f_N(x|\mu, h) = \frac{h^{1/2}}{2\pi} e^{-1/2 h(x-\mu)^2} \tag{13}$$

where

μ = mean value
h is known as the precision, and
$h = 1/\sigma^2$ or $\sigma = 1/\sqrt{h}$

If the size of the sample is ν, and successive values of x are generated, then the likelihood of finding the sample is equal to the product of the individual likelihoods

$$(2\pi)^{-1/2\nu} h^{1/2\nu} e^{-1/2 h\nu s^2} \tag{14}$$

where s = sample variance. For the normal data generating process, the following 3 cases are of interest: (a) true mean of the process is known; (b) precision of the process is known; and (c) the mean and the precision are unknown.

True Mean Known. —If the true mean of the process is known, then from Eq. 14, the sample likelihood is proportional to

$$h^{1/2\nu} e^{-1/2 h\nu s^2} \tag{15}$$

The natural conjugate to the kernel of the sample likelihood is the gamma - 2 probability distribution, which is

$$f_{\gamma_2}(h|s^2, \nu) = \frac{1/2\nu s^2}{(1/2\nu-1)!} (1/2\nu s^2 h)^{1/2\nu-1} e^{-1/2\nu s^2 h} \tag{16}$$

Eq. 16 leads to

$$h^{1/2\nu''} e^{-1/2 h\nu'' s''^2} \propto h^{1/2\nu'} e^{-1/2 h\nu' s'^2} h^{1/2\nu} e^{-1/2 h\nu s^2} \tag{17}$$

and

$$\begin{aligned} v'' &= \nu + \nu' \\ s''^2 &= \frac{1}{\nu}(\nu' s'^2 + \nu s^2) \end{aligned} \tag{18}$$

where the double prime denotes the posterior sufficient statistics, and the single prime the prior sufficient statistics.

Precision Known. —If the true mean is unknown, but the precision of the process is known, then the kernel of the likelihood is given by

$$e^{-1/2 hn(\bar{x} - \mu)^2} \tag{19}$$

where n = number of x's observed. The natural conjugate of the kernel of the sample likelihood is the normal distribution, and the distribution function of μ is given by

$$f_N(\mu|\bar{x}, hn) \propto e^{-\frac{1}{2}hn(\mu - \bar{x})^2} \tag{20}$$

Using the same symbology for prior, posterior and sample parameters, the following relationships are obtained:

$$\begin{aligned} n'' &= n' + n \\ n\,\bar{x}'' &= n'\bar{x}' + n\bar{x} \end{aligned} \tag{21}$$

True Mean and Precision Unknown. —If both the true mean and precision of the process are unknown, then the kernel of the likelihood is given by

$$\frac{(hn)^{\frac{1}{2}}}{2\pi}\, e^{-\frac{1}{2}hn(\bar{x} - \mu)^2}\, h^{\frac{1}{2}(n - 1)}\, e^{-\frac{1}{2}h(n - 1)s^2} \tag{22}$$

Raiffa and Schlaifer show that the natural conjugate is the normal-gamma distribution with $\nu = n - 1$

$$f_{N\gamma_2}(\mu, h|\bar{x}, s^2, n, \nu) = f_N(\mu|h, hn)\, f_{\gamma_2}(h|s^2, \nu) \tag{23}$$

The prior, posterior and sample parameters are related by the following expressions

$$\begin{aligned} n'' &= n + n' \\ \nu'' &= \nu + \nu' + 1 \\ n''\bar{x}'' &= n\bar{x} + n'\bar{x}' \\ \nu''s''^2 &= (\nu's'^2 + n'\bar{x}^2) + (\nu s^2 + n\bar{x}^2) - n''\bar{x}''^2 \end{aligned} \tag{24}$$

The marginal distribution of h as a random variable is gamma - 2, and the marginal distribution of μ is student.

Formulation of Pavement Design Process

The pavement design system previously formulated may be expressed in terms of the framework provided by statistical decision theory, and this involves the following steps:

1. Specify the prior probability distribution of the age at failure for each design, by the sufficient statistics.
2. Specify the conditional distribution of the surface deflection for each possible failure age, through the use of empirical or theoretical relations, for each design.
3. Estimate the distribution of the surface deflection of each design, and calculate the sample likelihood.
4. Calculate the posterior distribution of the age at failure for each design, either by the numerical or analytical procedures outlined above, for each design.
5. Calculate the present worth in dollars for each possible failure age, or establish the functional relationship between age and present worth.
6. Calculate the expected present worth of each design from the posterior probability distribution and the present worth relation.
7. Select that design with the minimum expected present worth.

The precise nature of each step will depend on the available theoretical and empirical models available. The analysis of a particular design problem may be carried out using either the preposterior or posterior modes of analysis. The mechanics of executing both these methods of analysis are well described by Raiffa and Schlaifer.

The procedure described above allows an objective and systematic comparison of possible solutions to a particular design problem. The framework which has been established is relatively free from the personal biases and immediate experiences of individual designers. Although the illustrative examples and criteria have been concerned with flexible pavements, any pavement type could be considered within this framework, as well as any parameter as a predictor of future pavement performance.

The application of this design procedure to the analysis of design decisions could be demonstrated by an example similar to that previously described. Instead of using discrete probability measures, the probability distributions could be specified, and the analytical approach described above used to evaluate the decision problem.

SUMMARY AND CONCLUSIONS

1. Current pavement design decisions are heavily biased by the personal experiences of individual designers, and the selection of an optimum solution to a pavement design problem is not always realized. No general framework has been established to date whereby systematic and objective comparisons of various pavement designs can be made.

2. The elements of a rational pavement design procedure have been established wherein both the technical and economic characteristics of designs, as well as the uncertainty of their future performance, are objectively accounted for.

3. The principles of statistical decision theory have been summarized, and the techniques for analyzing decision problems under uncertainty illustrated.

4. The pavement design system has been formulated in terms of the framework provided by statistical decision theory, and the steps basic to this formulation have been described. The framework allows an objective and systematic comparison of possible solutions to design problems which is relatively free from the personal biases and immediate experiences of individual designers.

REFERENCES

1. Gronberg, G. D., and Blosser, H. B. Lives of Highway Surfaces: Half Century Trends. Public Roads, June 1956.
2. Saskatchewan Department of Highways and Transportation. Road Life Study. Planning Branch Internal Report, Sept. 1962.
3. Canadian Good Roads Association. Pavement Evaluation Studies in Canada. Tech. Pub. No. 19, 1962.
4. Wilkins, E. B. Pavement Evaluation Studies in Canada. Internat. Conf. on the Structural Design of Asphalt Pavements Proc., 1962.
5. Benkelman, A. C., and Carey, W. N. Prediction of Flexible Pavement Performance from Deflection Measurements. AASHO Road Test, St. Louis. Conf. Proc. Highway Research Board, Spec. Rept. No. 73, 1962.
6. Campbell, G. D., and Wilkins, E. B. Flexible Pavement Design Based on Benkelman Beam Rebound Measurements. AAPT Proc., 1963.
7. Huculak, N. A. Maintenance Warrants Based on Pavement Evaluation. Canadian Good Roads Assn. Proc., 1963.
8. Luce, R. D., and Raiffa, H. Games and Decisions. John Wiley, N. Y., 1957.
9. Bross, I. D. J. Design for Decision. MacMillan Co., 1953.
10. Turkstra, C. J. A Formulation of Structural Design Decisions. Ph. D. Thesis, Univ. of Waterloo, 1962.
11. Tribus, M. The Use of the Maximum Entropy Estimate in Reliability. Recent Developments in Information and Decision Processes. Edited by R. E. Machol and P. Gray, 1962.
12. Tribus, M. Decision Theory and Design. Engineering Design Colloquim, Univ. of California, Los Angeles, 1962.
13. Raiffa, H. and Schlaifer, R. Applied Statistical Decision Theory. Graduate School of Business Admin., Harvard Univ., 1961.

Evaluating Highway Elevation Power Spectra From Vehicle Performance

B. E. QUINN, Professor of Mechanical Engineering, and
J. L. ZABLE, Graduate Student, School of Mechanical Engineering, Purdue University

A relatively new technique for describing the condition of a highway has been developed which consists of making a power spectral density analysis of elevation measurements obtained from the longitudinal pavement profile.

In calculating the elevation power spectrum it is necessary to make certain assumptions that influence the resulting spectrum. The question thus arises as to the validity of these assumptions.

A procedure is described in this paper that was used to obtain a pavement elevation power spectrum from dynamic tire force measurements. This involved the experimental determination of tire forces which were used as a criterion of vehicle performance.

The power spectrum obtained by this procedure is compared with power spectra calculated from elevation measurements (using different assumptions) to check the validity of the assumptions.

•VARIOUS INSTRUMENTS have been developed for evaluating pavement condition. Many of these devices, such as the BPR roughometer, obtain a number which is related to the roughness or smoothness of the highway profile. An investigator interested in predicting vehicle behavior (1, 2, 3) needs a more detailed description of the highway profile than is afforded by a measurement of this type. He needs a description of the highway that can be used with the vehicle characteristics to predict the behavior which he is studying.

Such a description can be obtained by making a power spectral density analysis of the longitudinal profile of a pavement (4). Unfortunately there is more than one way to make this analysis, and therefore different results can be obtained from the same data. It is the purpose of this paper to discuss this problem, and to suggest criteria by which the results of a power spectrum analysis of a highway profile can be evaluated.

THE HIGHWAY ELEVATION POWER SPECTRUM

Power spectrum analysis has been used extensively in electrical engineering problems for which the term "power" has an obvious meaning. When spectral analysis is employed in other areas the term "variance" would be more appropriate although it is rarely used. Either term refers to the mean square value of the variable being considered.

The result of applying power spectral analysis to highway elevation measurements is a curve showing the extent to which various wavelengths are present in the highway. In addition, the area under this curve is a measure of the roughness of the highway.

If a highway was perfectly level, perfectly smooth and at zero elevation, a power spectral density analysis of the elevation measurements would result in a curve that

Paper sponsored by Committee on Pavement Condition Evaluation.

would be a horizontal line coinciding with the horizontal axis shown in Figure 1. This curve would indicate that no undulations of any wavelength are present in the highway, and the area under this curve would be equal to zero (all the elevation measurements would be zero).

If, however, the highway at zero elevation was level and not perfectly smooth, but with randomly distributed undulations having wavelengths varying from L_1 to L_4, a power spectral density analysis of this highway would yield the curve shown in Figure 1. The total area under the curve would give the total mean square value (power) of the elevation measurements. Of considerable interest is the fact that the contribution to this mean square value from wavelengths ranging from L_2 to L_3 would be represented by the shaded area (Fig. 1). This area is usually referred to as the "power" associated with the wavelengths ranging from L_2 to L_3. It is this property that makes the curve attractive since the wavelengths that are significant can be identified. The curve also indicates that wavelengths longer than L_4 contribute nothing to the variation in the highway profile, and the same can be said for wavelengths shorter than those indicated by L_1. As a consequence only wavelengths between L_1 and L_4 are of any significance in the hypothetical highway under discussion.

In addition, another important property also exists. By using the curve shown in Figure 1, together with the appropriate vehicle characteristic, it is possible to predict the behavior of the vehicle on the highway. It is this latter property of the power spectrum curve that makes it very attractive to investigators interested in predicting vehicle behavior.

Although the wavelengths of undulations in a highway profile are easy to visualize and to discuss, they are not convenient to use in making power spectrum calculations.

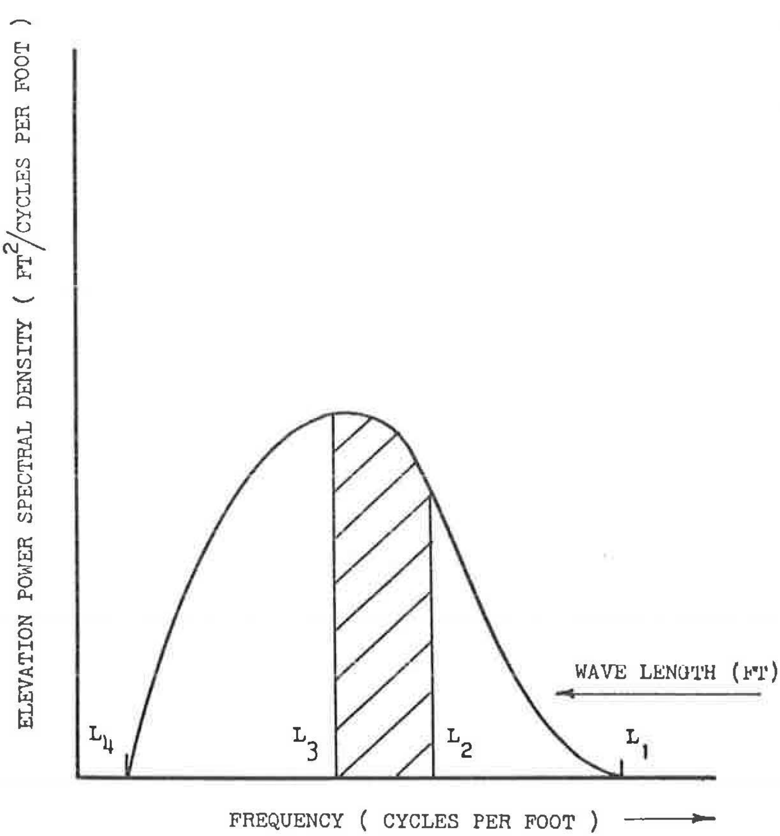

Figure 1. Elevation power spectrum for a hypothetical highway.

As a consequence a distance-based frequency is used in which frequency (in cycles per foot) is employed rather than wavelength. This quantity is the reciprocal of the wavelength and hence is easily related. The ordinate of the highway elevation power spectrum is in units of feet squared per cycle per foot and these units come naturally from the mathematical calculation. The area under the curve will therefore have the units that result when ordinate and abscissa are multiplied together. The resulting units are those of feet squared which would be associated with the mean square value of the elevation measurements.

It is not possible from a power spectrum curve to identify the amplitude of a single wavelength. Instead, it is possible to determine the mean square value of a range of wavelengths such as previously discussed.

A highway elevation power spectrum is therefore a curve. Information for calculating the ordinates of this curve can be obtained from either elevation measurements of the longitudinal profile, or from data obtained by a device that is sensitive to the highway profile.

The elevation power spectrum curve for a rough highway will have larger ordinates and a larger enclosed area than the power spectrum for a smooth highway. In addition, those wavelengths that contribute to the roughness can be easily identified. These properties, together with the fact that this characteristic can be combined with the vehicle characteristics to predict vehicle performance, make the power spectrum a valuable tool for the solution of certain highway problems.

The computational procedure for calculating a power spectrum is not included in this paper since such information can be obtained elsewhere (5).

COMPUTATION PROBLEMS

One of the problems involved in making a power spectral density analysis of a highway profile arises from the enormous range of wavelengths present in most highways. If a highway goes over a hill and down into a valley, a wavelength of several miles may exist that will have an enormous amplitude. On the other hand, extremely small wavelengths having very small amplitudes exist in a rigid highway in the form of brush marks in the concrete. In making a power spectral analysis it is therefore important to select that range of wavelengths that is significant for the problem at hand, and to make the analysis so that these wavelengths can be carefully studied.

Since "power" is related to amplitude, it is possible to estimate roughly the relative power of different wavelengths (a hill as compared to brush marks) by considering their respective amplitudes.

Selecting the wavelengths of interest usually involves more than just a consideration of amplitude. In a previous paper (3) those wavelengths were identified that were significant in determining the dynamic tire forces created by a passenger vehicle as it traveled over a highway. This required a knowledge of the natural frequencies of the vehicle suspension system as well as the selection of a vehicle velocity.

In general, wavelengths in the highway ranging from 4 ft to approximately 100 ft in length were found to be significant. Wavelengths within this range are therefore considered significant.

The horizontal distance between adjacent elevation measurements must be selected before the rod and level survey can be conducted. Many factors influence this decision and different investigators have used different distances. In all surveys conducted for the authors a distance of 1 ft has been used.

As the horizontal distance between elevation measurements is increased, the ability to measure the power associated with the shorter wavelengths is lost. This power is not eliminated from the analysis, but will appear in the power spectrum and will be erroneously attributed to other wavelengths (aliasing).

A problem of paramount importance in calculating a highway power spectrum from elevation measurements is that of removing the effects of very long wavelengths having large amplitudes (and power) such as are introduced by a hill and a valley. Moreover, if the highway is not at sea level the undesirable effect of an infinite wavelength is introduced. Long wavelengths are very undesirable because they generally distort the measurement of the power that is associated with the shorter wavelengths. Since these effects are all contained in elevation measurements it is virtually impossible to calculate a satisfactory highway elevation power spectrum directly from elevation data.

One method for dealing with this problem is illustrated in Figure 2. The original grade line of the highway is a section of a very long wavelength having a large amplitude. This was the original pavement profile when the pavement was perfectly smooth, and at that time the ordinates (and hence the area) of the power spectrum would ideally have been equal to zero. After years of use the pavement surface changed, and the present profile is represented by the irregular curve. If the highway power spectrum calculation is based upon the deviation of the present profile from the original grade line it will provide a measurement of the present roughness of the pavement. One problem, therefore, is determining these deviations accurately.

Different investigators have approached this problem in different ways. For this reason alone it is possible to obtain different power spectra from the same set of elevation measurements. One purpose of this paper is to indicate how the behavior of a vehicle can provide criteria whereby the "correct" technique can be identified.

Two techniques for determining the deviations of the pavement profile from the original grade line of the highway are discussed. In one method the first step is to obtain the average elevation $\overline{Y}$ from the entire set of elevation measurements Y_i. This value is then subtracted from each elevation measurement in turn to obtain the values indicated by Z_i. A running mean, established by a selected number of these quantities, is then subtracted from the value of Z_i at the midpoint of this mean to obtain the deviation X_i (Fig. 2). The values of X_i are then used to calculate the power spectrum.

The other technique for calculating X_i uses the values of Z_i as previously determined. In this case a second-order curve is fitted to the values Z_i by the least squares technique, and this curve is considered to represent the original grade line of the highway. The ordinate of this curve at each station is subtracted from the corresponding value Z_i to obtain the value of X_i. These values of X_i are then used to calculate the power spectrum.

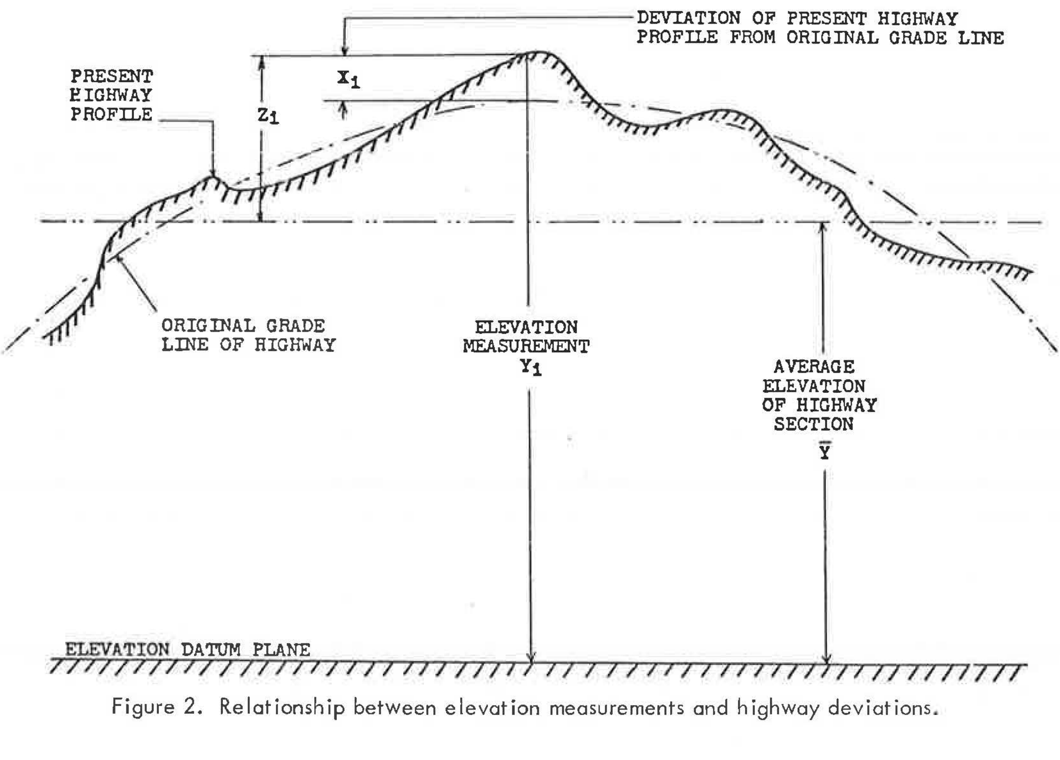

Figure 2. Relationship between elevation measurements and highway deviations.

The values of X_i obtained by these 2 methods will not be identical, and thus different power spectra will be obtained from the same set of elevation measurements Y_i. Moreover, additional techniques have been employed by other investigators to obtain values of X_i from the elevation measurements.

Investigators familiar with spectral techniques may indicate that data prewhitening procedures should be based primarily on a consideration of the entire frequency domain spectrum, and that these considerations should dictate the prewhitening procedure to be used. It should be recognized, however, that decisions concerning frequency domain filters also require the exercise of judgment, and that differences of opinion in this matter may also exist, giving rise to different spectra from the same basic data.

Another problem encountered is that of determining the appropriate length of highway to be used in this type of analysis. In general it is desirable to have as long a length of highway as possible, but physical and economic considerations often limit the length of the test section that can be considered. Generally speaking, the longer the length of highway that is analyzed the more statistically reliable will be the resulting calculations. A compromise is thus involved between statistical reliability and the number of elevation measurements that can be made. Such a compromise will also influence the power spectrum calculation.

The numerical technique whereby the power spectrum is calculated from the experimental data is also subject to personal judgment. It is not the purpose of this paper to go into great detail as to how these calculations are made but rather to discuss criteria whereby the validity of such calculations can be judged. In making the power spectrum calculation, however, it is necessary to calculate a relationship known as the autocovariance function. Such a function, when calculated, will consist of several ordinates plotted versus a distance parameter. One problem associated with this part of the calculation lies in the selection of the number of ordinates that will be used to represent the autocovariance function. More technically speaking, the maximum lag value that will be employed in generating this function is also a matter for individual judgment.

Without going further into mathematical details, there are other places in the calculation of a highway power spectrum in which discretion must be employed. Clearly a criterion is needed to evaluate the results of a calculation in which individual judgment must be exercised.

DETERMINATION FROM VEHICLE PERFORMANCE

The condition of a pavement will be reflected in the elevation measurements, as discussed. The pavement condition will also influence the behavior of a vehicle moving over the pavement. We shall now show how the performance of a vehicle can be used to obtain criteria by which the elevation power spectrum, calculated from elevation measurements, can be judged.

The performance of a vehicle moving over a pavement can be measured in many different ways. Some investigators measure vertical vehicle acceleration, some measure the relative displacement between the body and the unsprung mass of a vehicle and some measure strains in different parts of the vehicle. The measurement of vehicle performance used in this paper is the dynamic tire force, obtained by measuring changes in the air pressure in a tire as the vehicle travels over the pavement section under consideration (6). Other indications of vehicle performance can also be used, and it is possible that better results can be obtained if such are employed.

If a linear system experiences an input that can be characterized by a power spectrum, it is possible to calculate the corresponding power spectrum of the output (7). This technique requires the determination of a quantity known as a transfer function.

The transfer function of a system can be determined experimentally by subjecting the system to a sinusoidal input of known frequency and amplitude and determining the amplitude (and phase) of the output. Under these conditions the ratio of the amplitudes of the output and input is calculated, and this ratio is the value of the transfer function at the selected frequency. This process is repeated at different frequencies to obtain additional values for the transfer function.

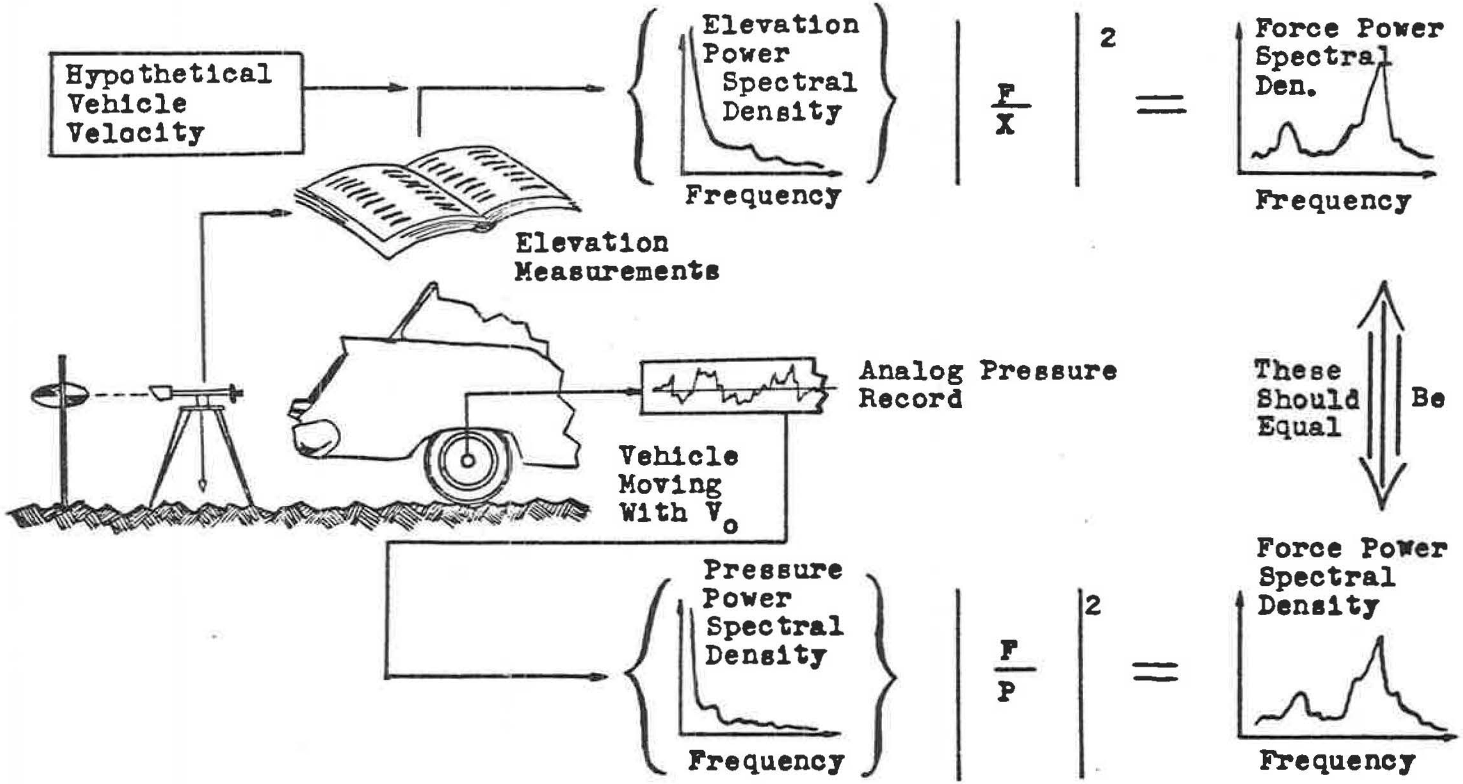

Figure 3. Two methods of calculating force power spectral density function.

The 2 transfer functions needed for this investigation are shown in Figure 3. The ratio F/P indicates that the force F on the tread of the tire is taken to be the output, while the differential air pressure P in the tire is the input. This relationship is necessary to determine the tire force from the tire pressure.

The other transfer function is shown by the ratio F/X. Here the output is the tire force F as previously, but the input is the displacement of the tread of the tire, represented by X. This relationship is necessary to determine the tire force from the highway elevation power spectrum.

The output power spectrum of a linear system is equal to the input power spectrum multiplied by the square of the transfer function. This process is shown in Figure 3 for 2 different inputs.

Considering first the problem of determining the dynamic tire force experimentally, records of tire pressure versus time can be determined experimentally from the vehicle moving over the highway. From these records it is possible to calculate a pressure power spectrum as shown by the arrow (Fig. 3). The tire pressure is related to the tire force, and this relationship (F/P) can be determined experimentally in the laboratory. The power spectrum of the dynamic tire force can be computed by multiplying the pressure power spectrum by the relationship between the tire force and the tire pressure (Fig. 3). As may be expected, certain assumptions are also involved in computing the pressure power spectrum. There is one large difference, however, between making this calculation and computing a power spectrum from elevation measurements. This difference arises because there are no long wavelengths present in the tire pressure measurements, such as in the elevation measurements; therefore, the pressure power spectrum can be computed with greater accuracy than the elevation power spectrum.

It is also possible to compute the dynamic tire force theoretically. If elevation measurements are made of the highway in question then it is possible to compute an elevation power spectrum. (It is this relationship that introduces the greatest error because of the problems inherent in this calculation.) If the relationship (F/X) between tire force and tire displacement is known, it is possible to calculate the force power spectrum from the elevation power spectrum (Fig. 3). This force power spectrum should check with the one obtained from the experimental pressure measurements.

A comparison of these force power spectra thus provides a criterion whereby the accuracy of the elevation power spectrum can be judged.

Since the vehicle characteristics have been determined, it is possible to start with the tire pressure spectrum and determine an elevation power spectrum. First, the force power spectrum is obtained from the experimental tire pressure measurements. The vehicle characteristics in the form of the F/X ratio are then removed, and an elevation power spectrum results. This is the elevation power spectrum experienced by the car, and it should be the same as that calculated from the elevation measurements. A direct comparison can thus be made of the 2 elevation power spectra, and the accuracy of the spectrum computed from elevation measurements can be judged by using as a criterion the spectrum obtained from the vehicle performance.

The question may be raised whether the relationships between tire force and tire displacement and between tire force and tire pressure are affected by the speed of the vehicle. Laboratory tests indicate that the amplitude of the vehicle motion will influence these characteristics as will the magnitude of the applied forces. Thus these ratios, so important in the calculation of the desired power spectra, are themselves subject to change. This is to be expected since the vehicle suspension system is nonlinear. How much do these characteristics change, and are changes in one characteristic compensated by changes in another?

As an initial check on these questions, it was decided to run the test vehicle at different speeds on the same length of highway. In all cases the vehicle would be excited by the same highway profile and the elevation power spectrum should be the same at all speeds. Increasing the vehicle velocity would, however, increase the magnitude of the applied forces and hence at different speeds different tire pressure records would be obtained. To what extent would consistent behavior be observed on the part of the vehicle?

Figure 4 shows the results of this initial test, in which the vehicle was operated at speeds of 30, 40, 50, and 60 mph over the same length of highway. The curves indicate that the elevation power spectrum experienced by the vehicle is virtually the same at speeds from 40 to 60 mph, but at 30 mph there is some deviation. However, the close agreement in the results was gratifying because there were many possibilities for error. As a result of these tests it was decided to operate the vehicle in the range of 40 to 60 mph since a slight change in vehicle velocity would have relatively little effect on the resulting elevation power spectrum.

Appropriate highway sections were selected and elevation measurements were obtained. Elevation power spectra were then computed from these elevation measurements by using the 2 different techniques for obtaining elevation deviations previously

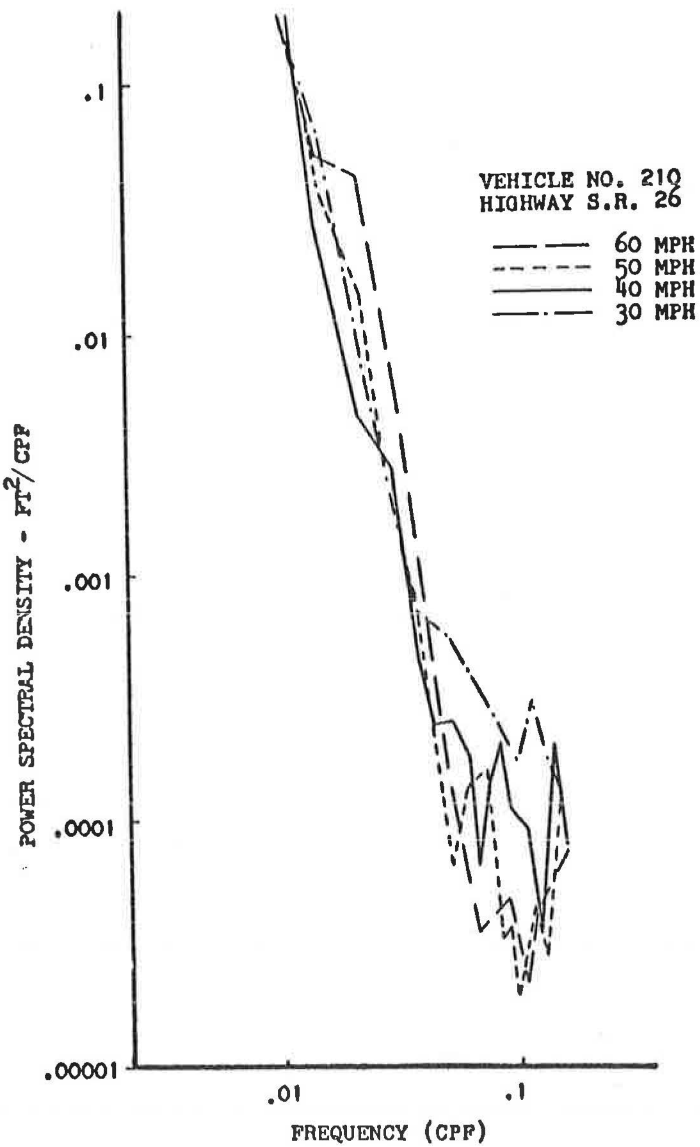

Figure 4. Elevation power spectra experienced by the vehicle at various speeds.

discussed. Typical results are shown in Figure 5 where the power spectrum curves indicate that the greatest amount of power is found in the long wavelengths. This means that long wavelengths in the highway provide the greatest excitation for producing vertical motion in the vehicle.

The curves (Fig. 5) indicate that different power spectra are obtained from the same set of elevation measurements if different procedures are used to obtain the elevation deviations. This is shown by the uppermost curve, for which the elevation deviations were obtained by merely subtracting the mean of all elevation measurements $\overline{Y}$ from each value of elevation Y_i. (In other words the values of Z_i were used in place of the values for X_i in this calculation.) The curve shown by the solid line is the elevation power spectrum actually experienced by the vehicle, determined from the dynamic tire pressure measurements.

When the elevation power spectrum is calculated from the tire pressure measurements, large values for the power spectrum are also obtained (Fig. 5) at the longer wavelengths (low frequencies). This occurs because the ratio between tire force and tire

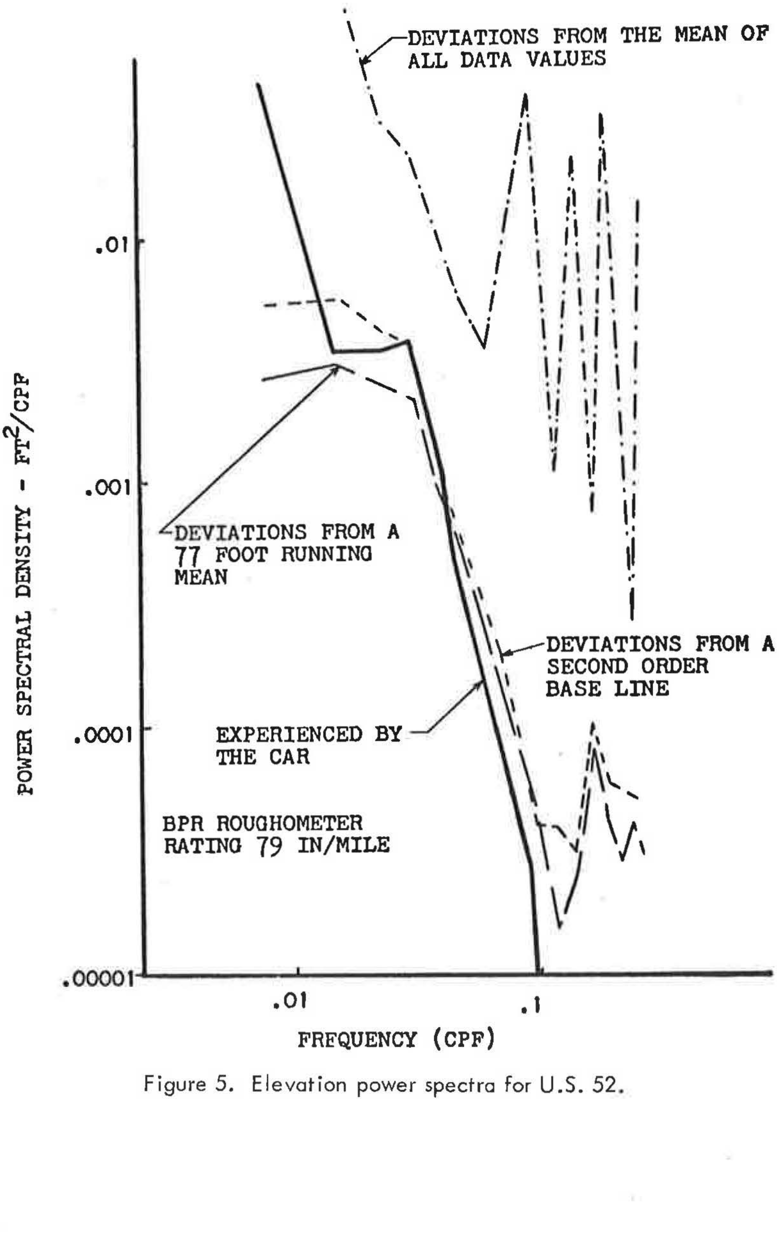

Figure 5. Elevation power spectra for U.S. 52.

displacement approaches zero as the frequency decreases. Hence, at low frequencies it is necessary to divide the ordinates of the dynamic tire force spectrum by values which are very close to zero. As a consequence the elevation power spectrum experienced by the car (obtained from dynamic tire force measurements) displays the same characteristics as the power spectra calculated from the elevation measurements. This is gratifying in terms of the trend shown, but it is difficult to compare numerical values in the low frequency region since each procedure is subject to limitations.

The power spectrum experienced by the car thus affords the criterion whereby the power spectra calculated from elevation measurements can be compared, but this comparison is confined chiefly to the higher frequency region. Since a large amount of power is found in the lower frequency region, this criterion leaves something to be desired. Nevertheless, it indicates that for the highway shown, deviations obtained from either the running mean or a second-order least squares base line yield a result close to that experienced by the vehicle. In addition, the power spectrum calculated

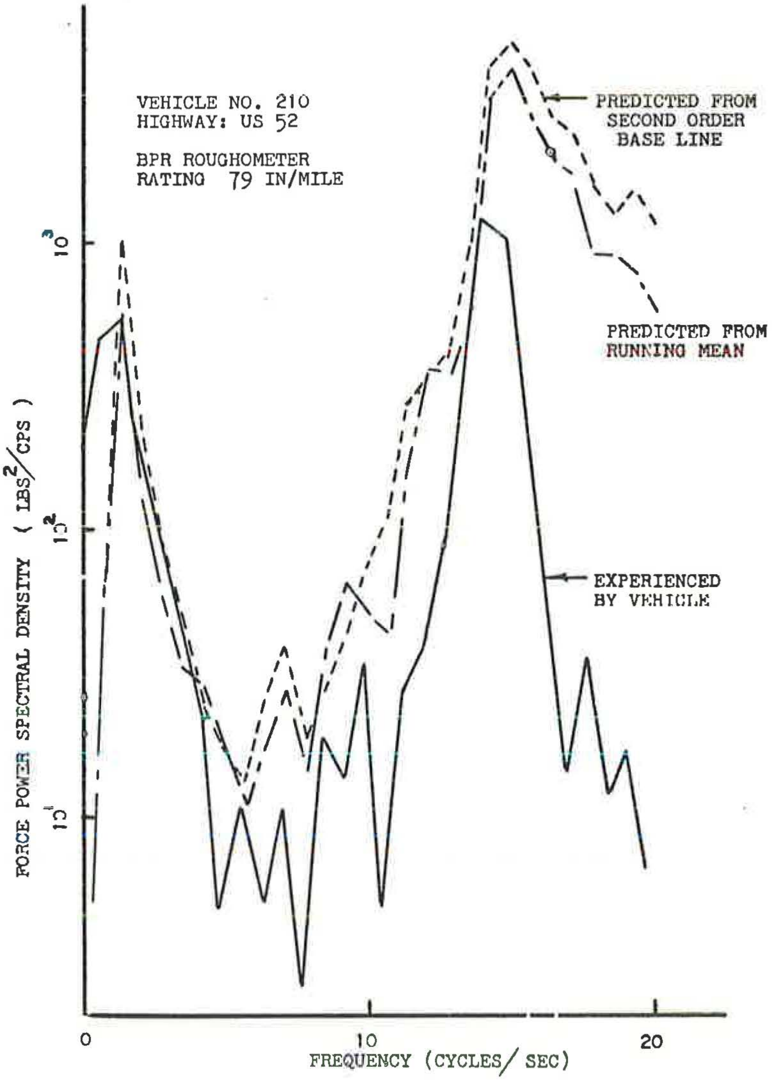

Figure 6. Comparison of force power spectra.

from the mean of all data values is based on a procedure which does not yield a highway characteristic comparable to that experienced by the vehicle.

Figure 5 also shows that at frequencies in excess of 0.1 cpf (wavelengths less than 10 ft) the power spectra calculated from elevation measurements overestimate the amplitudes of the existing undulations. This cannot be ignored, because certain vehicles are very sensitive to these wavelengths at normal operating speeds, and the use of these power spectra will result in predicted vehicle behavior that will be in excess of that encountered in actual operation.

One cause of this overestimation is the limited accuracy with which the elevation measurements were made; other factors in the calculation procedure also contribute to this error.

The existence of a large amount of power in the first frequency band is disturbing, and it is difficult to compare power spectra when the first band is included in the power calculation. It has been shown (3), however, that the vehicle is relatively insensitive to highway excitation at low frequencies, and hence a large amount of power in the highway at low frequencies does not necessarily result in a prediction of excessive forces generated by the vehicle. Keeping this in mind, it is instructive to examine the force power spectra computed from the elevation measurements and the vehicle characteristics (F/X) compared with the force power spectrum determined experimentally from the tire pressure measurements (Fig. 6).

The force power spectrum, determined from the tire pressure measurements, indicates that 2 frequencies predominate in the vehicle behavior. The lower frequency at which appreciable forces are generated is a result of the motion of the sprung mass of the vehicle (body roll) and is indicated by the peak in the curve near 2 cps. The peak in the region of 14 cps indicates that large forces are induced that result from the motion of the unsprung mass of the vehicle (wheel hop).

The force power spectra predicted from both elevation power spectra indicate larger forces in the high frequency region than actually exist. This is a direct result of the higher values of the elevation power spectra computed from elevation measurements (Fig. 5).

Thus a highway elevation power spectrum, computed from elevation measurements, can be used with the proper vehicle characteristics to obtain the corresponding force power spectrum (Fig. 3). This can be checked with the force power spectrum determined from the tire pressure measurements, and this comparison can serve as a criterion of the accuracy of the elevation power spectrum obtained from elevation measurements.

A comparison of force power spectra, rather than of elevation power spectra, offers the advantage of curves that have a better-defined area in the low frequency region. In addition, the response of the vehicle serves to define the range of frequencies that is important, and in this way the range of wavelengths can be identified that is significant in the highway profile.

Although the results shown in Figures 5 and 6 pertain to only one highway, similar calculations have been made for other highways. In most instances the results have been very similar, and in all cases the predicted forces were larger than those measured experimentally (Fig. 6).

In general, these calculations can be made with greater accuracy for smooth highways than for very rough ones. Moreover, best results to date have been obtained for rigid and flexible highways, rather than for those of overlay construction.

CONCLUSIONS

The elevation power spectrum of a highway can be determined from the performance of a vehicle as well as from elevation measurements. The performance of the vehicle was taken to be the dynamic tire force, but other vehicle performance characteristics such as stress or acceleration could also be used.

Results indicate that elevation deviations obtained from either second-order least squares base lines or from a running mean produce an elevation power spectrum from highway elevation measurements that is in many ways reasonably close to that experienced by the vehicle. (Introducing the corresponding frequency domain filters will improve the results but will not resolve the basic problems encountered at both the high and low frequencies.) In both cases, however, the tendency is to overestimate the high frequency (short wavelength) effects. In the case of dynamic tire forces, the vehicle is very sensitive at these frequencies and hence an even greater overestimation of the forces results. This is partly due to the accuracy with which elevation measurements can be made, and partly to the procedures used in making the power spectrum calculations.

Therefore, it appears that more accurate characterizations of highway profiles can be obtained by observing the performance of a device with appropriate response characteristics as it moves over the highway profile in question than can be obtained from elevation measurements made under normal conditions. In checking the performance of such a device, however, the elevation measurements are very useful.

ACKNOWLEDGMENTS

The support of the Bureau of Public Roads through Contract CPR 11-7941 is gratefully acknowledged. Assistance was also received from the Joint Highway Research Project at Purdue University and from the Indiana State Highway Commission. Some data used in this analysis were also obtained from National Cooperative Highway Research Project 1-2.

REFERENCES

1. Grimes, C. K. Development of a Method and Instrumentation for Evaluation of Runway Roughness Effects on Military Aircraft. AGARD Report 119, May 1957.
2. Houbolt, J. C. Runway Roughness Studies in the Aeronautical Field. Journal of the Air Transport Division, ASCE Proc., Vol. 86, No. AT 1, March 1961.
3. Quinn, B. E., and Thompson, D. R. Effect of Pavement Condition on Dynamic Vehicle Reactions. Highway Research Board Bull. 328, 1962.
4. Walls, J. H., Houbolt, J. C., and Press, H. Some Measurements and Power Spectra of Runway Roughness. NACA TN 3305, 1954.
5. Blackman, R. B., and Tukey, J. W. The Measurement of Power Spectra. Dover, 1958.
6. Wilson, C. C. A Dynamic Tire Force Measuring System. Joint Highway Research Project Report No. 6, Purdue University, March 1964.
7. Lanning, J. H., and Batten, R. H. Random Processes in Automatic Control. McGraw-Hill, 1956.

GMR Road Profilometer—A Method for Measuring Road Profile

ELSON B. SPANGLER and WILLIAM J. KELLY
Engineering Mechanics Department, Research Laboratories, General Motors Corporation

Accurate road profiles are often required for the analytical study of vehicle ride and vibration phenomena induced by road irregularities. The desire to bring profiles of existing roads into the laboratory has led to the development of a road profilometer for the rapid measurement of such road profiles. The continued interest in this device by persons engaged in highway design, construction and maintenance encouraged the authors to further develop and simplify this instrument and to make it available to these highway groups. This paper discusses the basic operating principle of the GMR profilometer, describes the unit supplied to the Michigan State Highway Department, and presents some typical test results.

•AN AUTOMOBILE riding on a road can be considered a complex mechanical filter. The vertical displacements introduced at the tire contact patch are drastically modified by the filtering action of the tire, suspension, frame, body mounts, body and seat before they reach the passenger. To assist in the analytical and experimental study of vehicle ride, the GMR road profilometer has been developed to produce accurately measured road profiles to be used as an input into the simulation of this complex filter. An earlier profilometer (1) physically established a reference which was used to measure the displacement of a road-following wheel. This system involved an analog computer, a hydraulic system and two cumbersome trailers on the rear of the towing vehicle. In the new GMR road profilometer, the road-following wheels are located under the towing vehicle, the hydraulic system has been eliminated, and the analog computer has been replaced by an inexpensive analog computation package. During the development work, the Research Laboratories worked closely with highway engineers, both at the General Motors Milford Proving Ground and in other highway engineering groups. A by-product of this activity was the request by highway engineers that the GMR road profilometer be made available for their use. As a public service, the authors have assisted the Michigan State Highway Department in a Bureau of Public Roads research project to evaluate the GMR road profilometer for highway department use.

MECHANICAL VIBROMETER

One of the principal problems in measuring road profile with reasonable flexibility and speed is establishing a reference from which to measure deviations. Optical systems such as used in surveying and light beam references are slow and not readily applicable to curved roads. In addition, it is desirable to obtain a continuous record for ride simulation purposes. After consideration of many alternative possibilities, a system with an inertial reference was chosen for development. This system has the

Paper sponsored by Committee on Pavement Condition Evaluation.

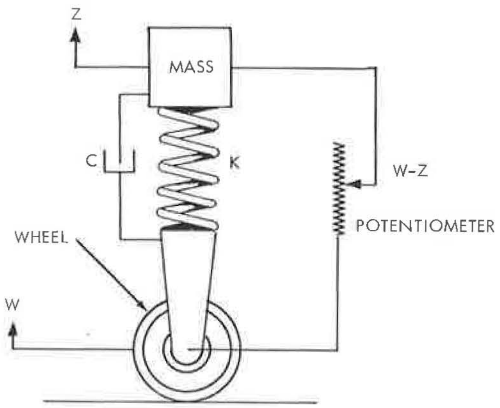

Figure 1. Mechanical vibrometer.

ability to measure the range of road wavelengths significant to vehicle ride. The principle of the inertial reference system is illustrated by the mechanical vibrometer (Fig. 1). At very low frequencies the motion of the mass follows the wheel motion, but at higher frequencies the motion of the mass is small and the relative motion between the wheel and mass (W-Z) is essentially the road profile. This simple mechanical filter can be described by a block diagram (Fig. 2), where the road profile or wheel displacement W enters from the left. The output of the mechanical filter is the displacement of the mass Z. The potentiometer, represented in Figure 2 by a summer, measures the relative motion between the wheel and the mass to produce the output W-Z. The behavior of the mechanical vibrometer system is shown in the frequency response curve of Figure 3. (The analysis of the GMR profilometer is based on a frequency response approach; a brief discussion of frequency response is included in Appendix A.) This curve is for a system having a natural frequency of 6 rad/sec. Mechanical systems with natural frequencies lower than 6 rad/sec are difficult to design. Equivalent road wavelengths at different vehicle speeds are shown along the abscissa in addition to frequency. Shorter wavelength disturbances which produce frequencies above the natural frequency of the mechanical system can be measured by the relative displacement of the wheel and sprung mass. However, lower frequency components are attenuated.

MECHANICAL AND ELECTRONIC VIBROMETER

The road profile can be measured exactly with a mechanical vibrometer (Fig. 2) if the motion of the mass Z is measured and added to the measured motion $(W-Z)_m$. The motion of the mass can be determined from its acceleration by double integration. This is the operating principle of the GMR road profilometer as shown in the system block diagram (Fig. 4). The left side is recognized as the block diagram of the mechanical vibrometer. The remainder is the addition of an accelerometer, the double integration of the accelerometer signal to obtain the measured displacement of the mass Z_m, and the summation of $(W-Z)_m$ and Z_m to produce the measured road profile W_m.

Frequency response plots on a log-log scale of the individual operations (Fig. 4) aid in the understanding of the principles. The frequency response of the mechanical filter is shown in Figure 5. If for low frequencies (long wavelengths) the motion Z and the motion W could be measured from the same reference, the output of the mechanical filter Z would equal the input W. The amplitude ratio (Z/W) would be unity. As the frequency increases above the natural frequency of the mechanical filter ω_n, the motion of the mass Z becomes smaller than the input W. This frequency response curve is,

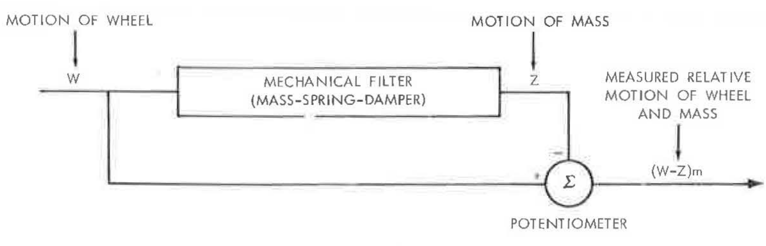

Figure 2. Block diagram of mechanical vibrometer.

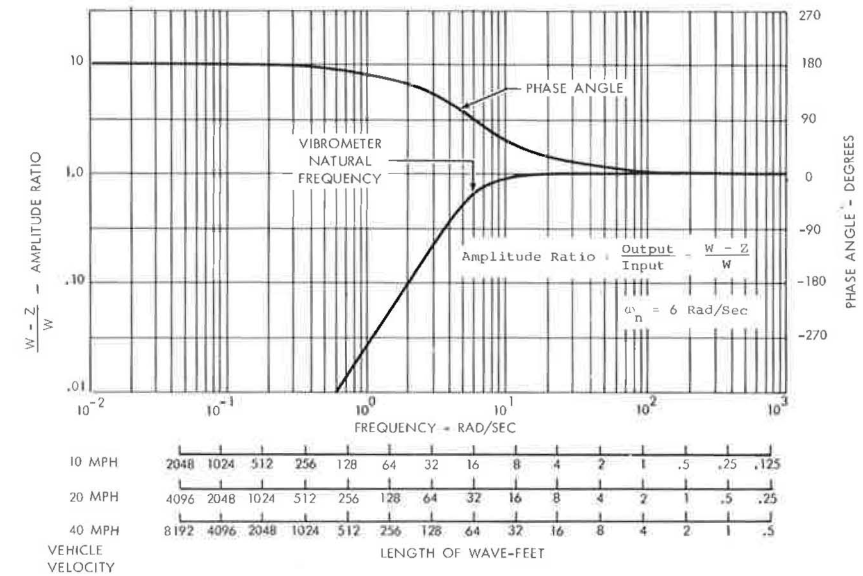

Figure 3. Frequency response of mechanical vibrometer.

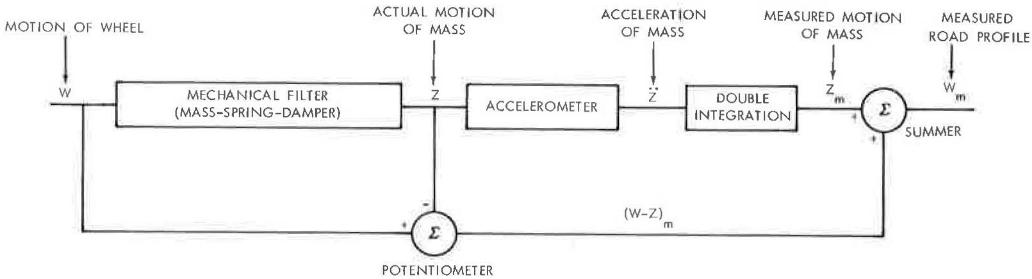

Figure 4. Block diagram of mechanical and electronic vibrometer.

of course, consistent with our observations as an automobile passenger. We have much less motion than the wheel and tire on short wavelengths (washboard road) but tend to go up and down with the wheel and tire on long wavelengths (hills and valleys).

The next element in Figure 4 is the accelerometer. This transducer converts displacement of the mass to its acceleration. An ideal accelerometer would have the characteristic plotted in Figure 6. The acceleration, for a fixed displacement amplitude, varies directly as the square of the frequency.

The frequency response of the double integration following the accelerometer (Fig. 7) is exactly the inverse of the accelerometer characteristic. The computed amplitude of the mass Z for a constant acceleration amplitude input varies inversely as the square of the frequency.

Figure 8 is the same block diagram as Figure 4 with the amplitude of the signals after each operation shown as a function of frequency. The measured road W_m theoretically exactly equals the real road W. The low frequency (long wavelength) road waves are reproduced through the accelerometer branch; the high frequency (short wavelength) road waves are detected by the potentiometer with the dividing point being the natural frequency of the mechanical filter ω_n.

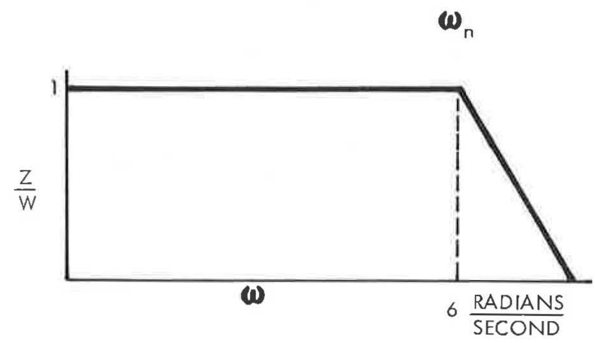

Figure 5. Frequency response of mechanical filter.

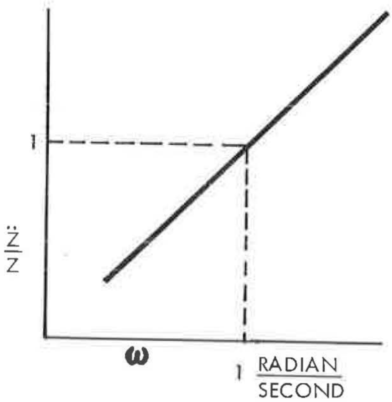

Figure 6. Frequency response of an accelerometer.

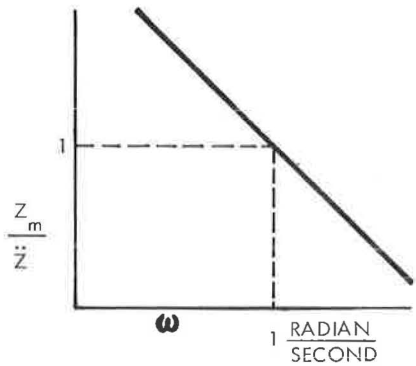

Figure 7. Frequency response of double integration.

HIGH PASS FILTER

The GMR profilometer is theoretically capable of measuring the road profile exactly at all frequencies. Practically, this is neither possible nor desirable for most applications. Usually, a person who is interested in road profile for vehicle ride or road condition purposes is not interested in the long wavelengths (hills and valleys). However, it is considered desirable to allow the user to determine what wavelength information he wants to collect. This is accomplished by use of a high pass filter which attenuates amplitudes at all frequencies below the filter frequency, ω_f. The frequency response for the high pass filter is shown in Figure 9. Adding a high pass filter to Figure 8 produces the block diagram of the complete GMR profilometer (Fig. 10). The operations of double integration, summation and filtering are enclosed and separated from the rest of the system (Fig. 10) by a box described as "analog computations." The inputs to the analog computation box are the transducer signals from the potentiometer and accelerometer. The output from the analog computation box is the filtered, measured road profile.

COMPLETE SYSTEM PERFORMANCE

For ease of explanation, the frequency response characteristics of the various signals in Figure 10 are represented by straight line approximations on log-log scales. The actual frequency response of the complete system is shown in Figure 11. The abscissa is again expressed as both frequency and wavelengths at various recording vehicle speeds. The amplitude is shown as a ratio of measured road profile W_f to the

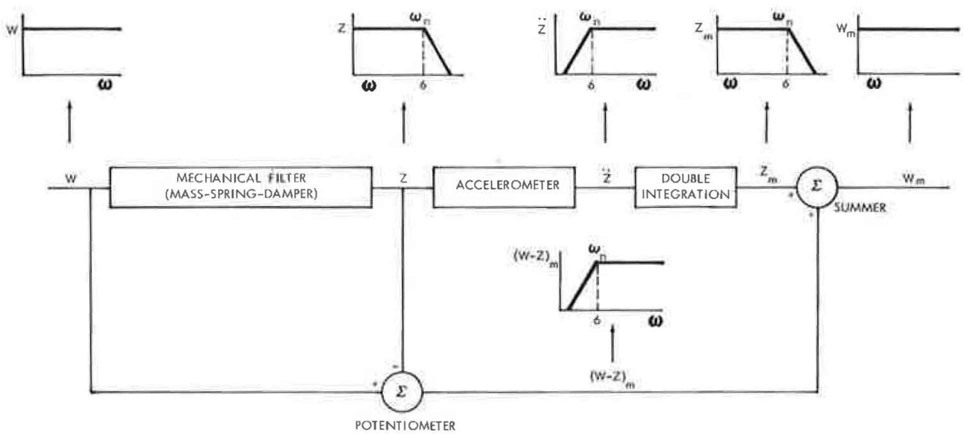

Figure 8. Block diagram of mechanical and electronic vibrometer.

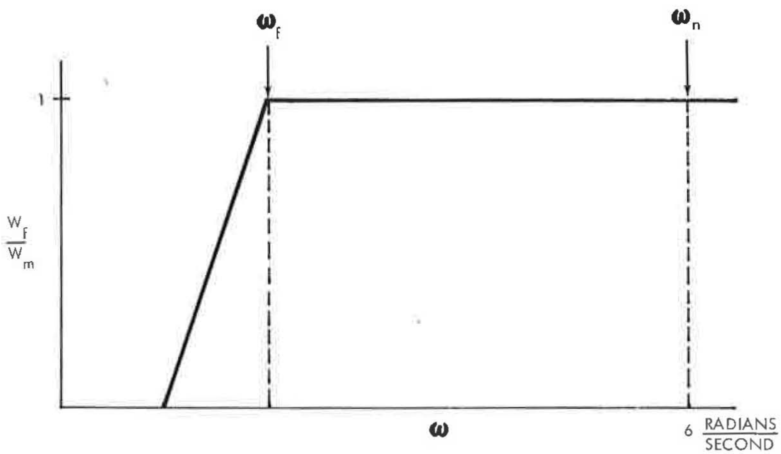

Figure 9. Frequency response of high pass filter.

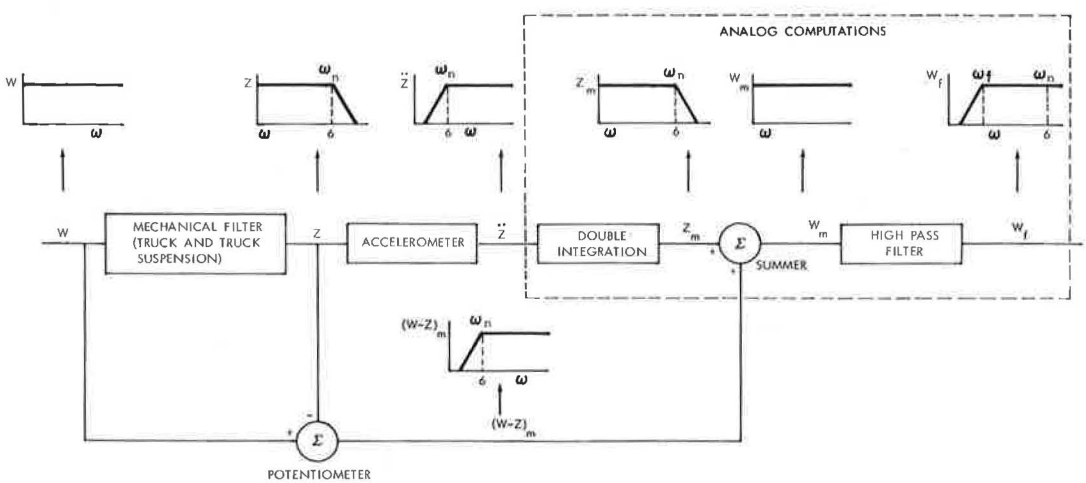

Figure 10. Block diagram of complete GMR profilometer.

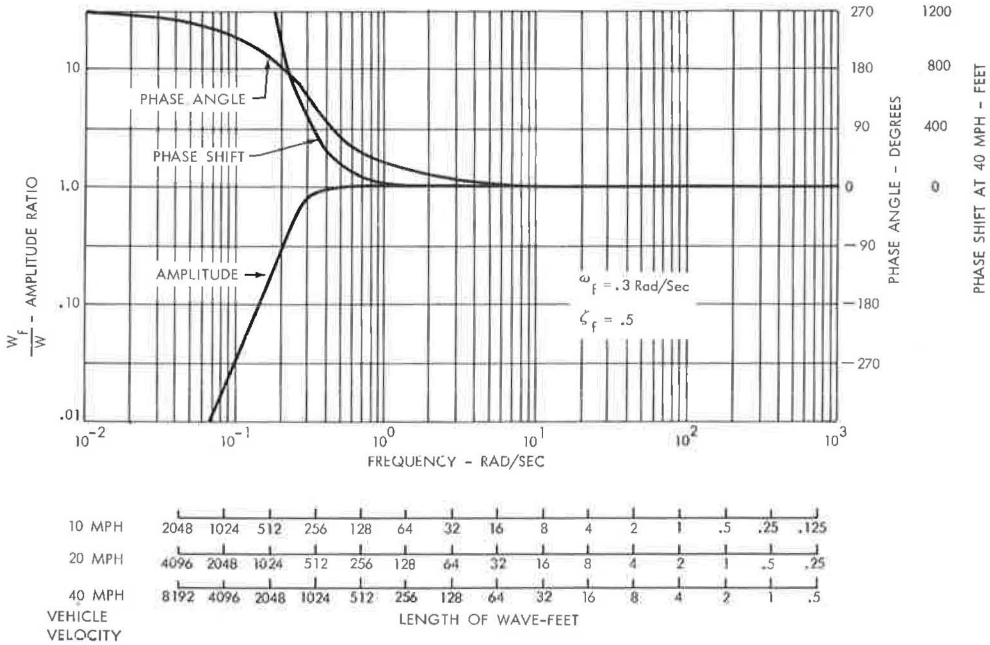

Figure 11. Frequency response of complete system.

actual road W. Note the similarity between the frequency responses of Figures 11 and 3. The response of the mechanical and electronic vibrometer is similar to the response of the mechanical vibrometer except that longer wavelengths can be measured with the former.

As an example of the influence of wavelength on amplitude, a 100-ft sinusoidal wave measured at 40 mph would be measured with an amplitude ratio of one (Fig. 11). The measured wave would have the same amplitude as the actual wave. However, the

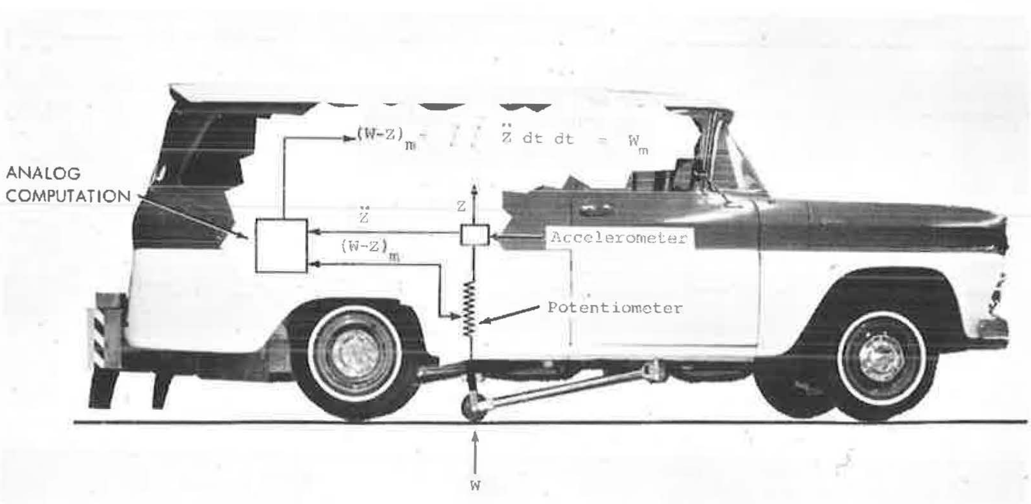

Figure 12. GMR road profilometer.

amplitude of a 2,000-ft sinusoidal wave would be measured with an amplitude of one-tenth its actual value. A second characteristic of the system is the measured road phase shift. In filtering, whether electronic or mechanical, the output of the system is shifted along the wave form or road profile from where it actually should be (Figs. 3 and 11). The attenuation and phase shift must exist if the hills and valleys are rejected by the measuring system. From Figure 11, there is practically no phase shift in the measurement of the 100-ft sinusoidal wave measured at 40 mph, but the 2,000-ft wave as measured leads the actual wave by 180°, half a wavelength or 1,000 ft. Normally, the 2,000-ft waves are not of interest. The wavelengths of interest are measured without amplitude change or phase shift. Figure 11 shows that higher recording vehicle velocity produces better fidelity. A 100-ft sinusoidal wave is measured at 40 mph with practically no phase shift but a phase shift of 45°, one-eighth of the wavelength, or 12 ft, is introduced if the recording vehicle velocity is 10 mph.

The selection of the filter natural frequency ω_f is based almost exclusively on the road amplitude and the road frequencies of interest. It would be desirable, of course, to have the filter natural frequency as low as possible at all times to provide accurate reproduction of all wavelengths. But, if the road being measured has large-amplitude, long-wave components, the voltage capacity of the analog computation components may be exceeded. This would suggest 2 courses of action. The filter natural frequency ω_f may be raised or the voltage scaling of the analog computation may be reduced. This latter course will result in reduced accuracy on small amplitude components. The flexibility to change quickly both filter natural frequency and analog computation scaling to suit requirements has been built into the GMR profilometer.

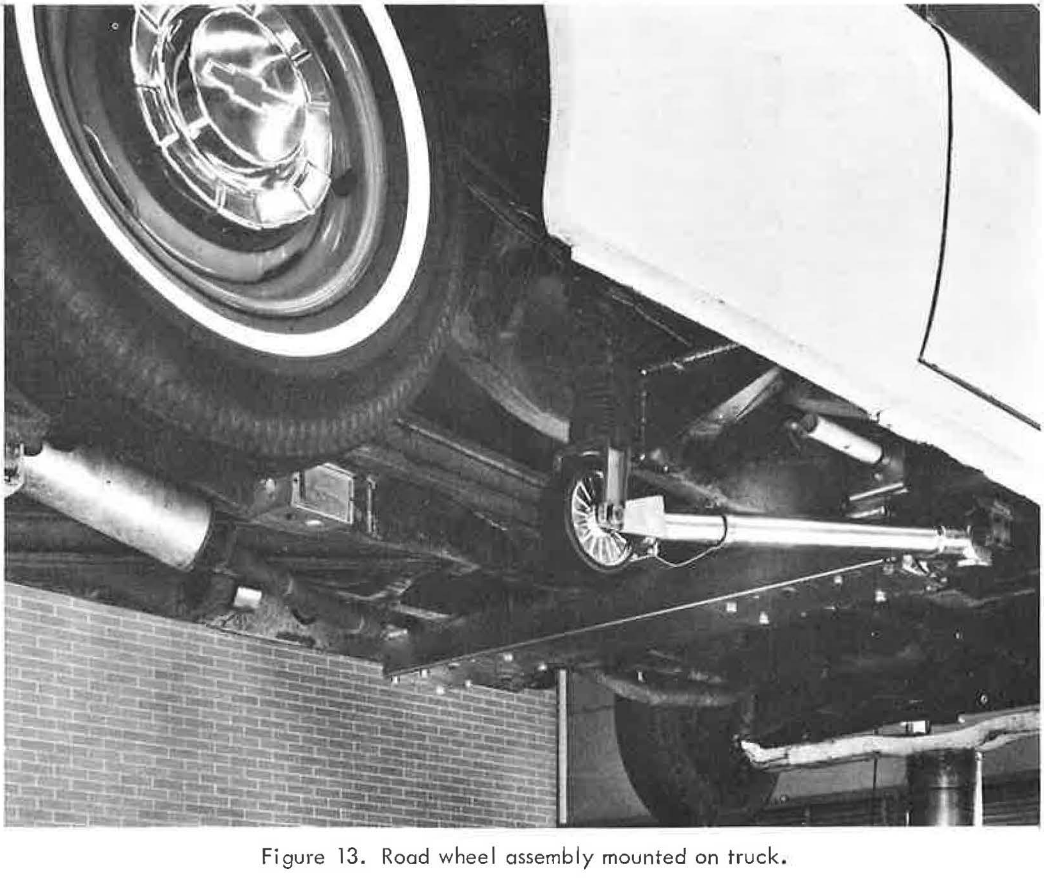

Figure 13. Road wheel assembly mounted on truck.

GMR ROAD PROFILOMETER

The road wheel of the GMR road profilometer (Fig. 12) is mounted on a trailing arm underneath the measuring vehicle. The wheel is held in contact with the ground with a 300-lb spring force. The truck mass and truck suspension form the mechanical filter between the road and accelerometer. The relative motion of a location on the vehicle body and the road wheel $(W-Z)_m$ is measured with a potentiometer. The accelerometer is mounted on the vehicle body above the road-following wheel at the point where the potentiometer fastens to the body. The 2 signals $(W-Z)_m$ and $\ddot{Z}$ are inputs into an analog computer; the output is W_m.

Road Wheel Assembly

The wheel and wheel hold-down mechanism are mounted under the measuring vehicle on the frame (Fig. 13). Figure 14 shows the general arrangement of the parts in the assembly. The road wheel is supported on a trailing arm which is free to rotate about a transverse axis located in a transverse tube which attaches to the vehicle. A torsion bar applies a torque from the transverse tube to the trailing arm to keep the road wheel in contact with the road surface. A kingpin in the trailing arm allows for misalignment and prevents scrubbing of the road wheel during turning maneuvers.

The road wheel (Fig. 15) is a lightweight, small-diameter wheel with a thin natural-rubber tire. The considerations in selecting the small wheel size are (a) a small wheel is easier to keep in contact with the ground than a wheel with more mass, (b) a small wheel performs less geometric filtering on the road profile than a large wheel,

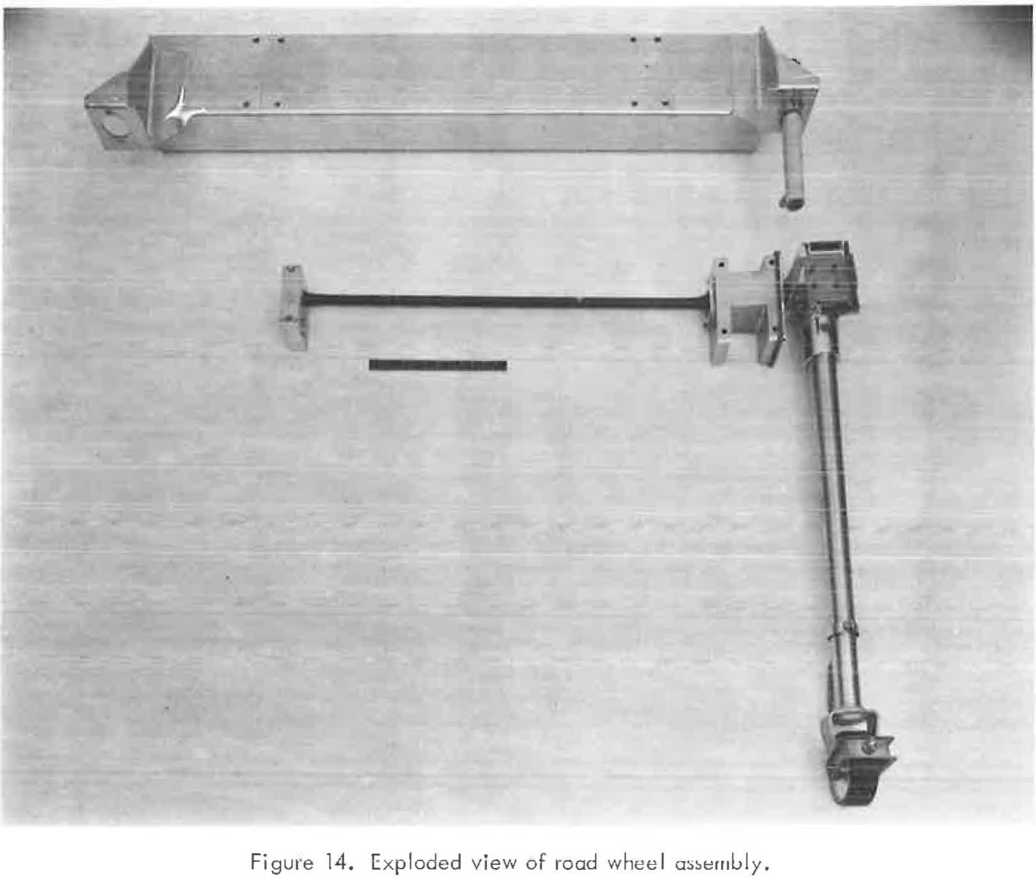

Figure 14. Exploded view of road wheel assembly.

and (c) the signals due to wheel out-of-roundness will introduce errors at shorter wavelengths. The shorter wavelength disturbances in the road do not excite appreciable vehicle vibrations and introduced errors may be disregarded.

A small road wheel also has several disadvantages. The wheel is small enough to get lost in a pothole in the road and be pulled off the towing vehicle. To overcome this difficulty, a skid is mounted on the trailing arm that will allow the wheel to drop no lower than 1.75 in. below a point 5 in. ahead of the wheel centerline (Figs. 13 and 14). A second difficulty is the high rotational speed, which is approximately 2260 rpm at 40 mph. The factors which dictated the choice of a thin natural-rubber tire molded to the wheel rim are (a) wear, (b) high temperature bond strength, and (c) low hysteresis which results in a lower operating temperature.

Figure 16 shows the recorded wheel displacement resulting from a wheel passing over a wedge at 40 mph. The natural frequency of 80 cps of the wheel and wheel hold-down system can be determined by the number of wheel bounces per unit time after the wheel has passed over the wedge. At a vehicle recording speed of 40 mph, wheel bounce would produce waves approximately 9 in. long. This low-amplitude, short-wavelength wheel bounce will not interfere with any road profile analysis presently contemplated.

A hydraulic piston and lever arrangement allows the road-following wheel to be raised off the ground when not in use. The vehicle driver controls this with a hand pump or the switch of an electric motor-driven pump. This accessory makes possible the rapid transit from one test site to another without concern about the road wheel.

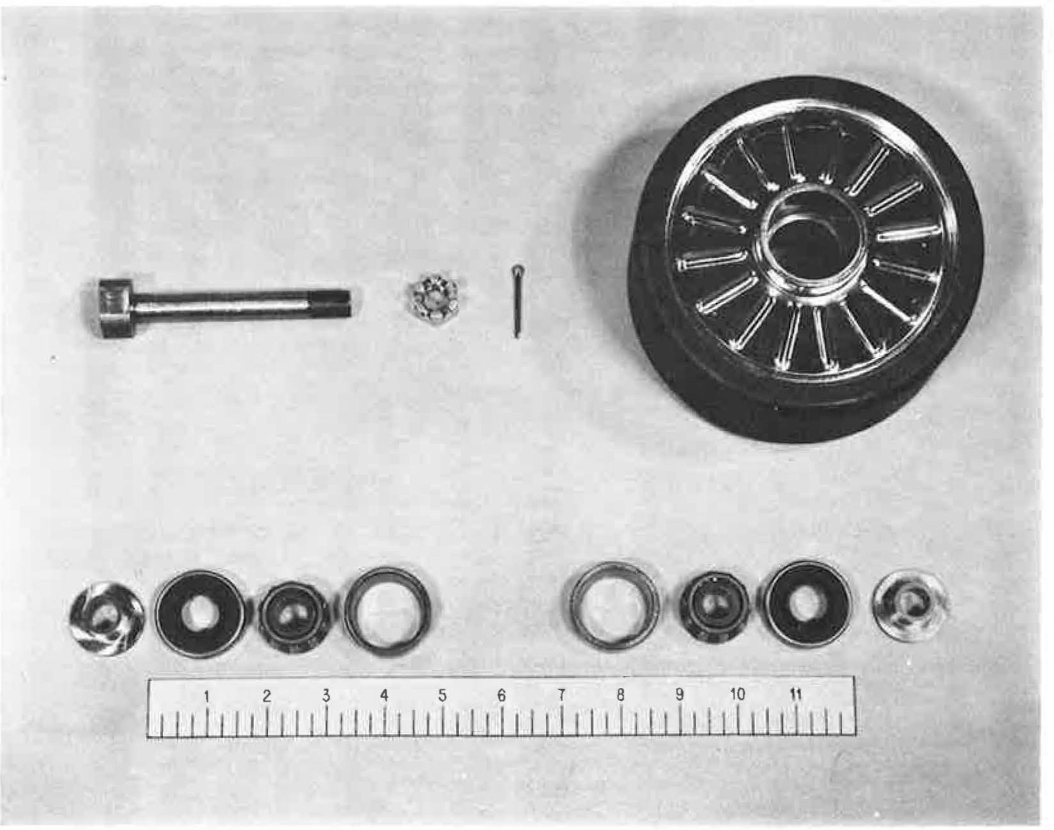

Figure 15. Road wheel.

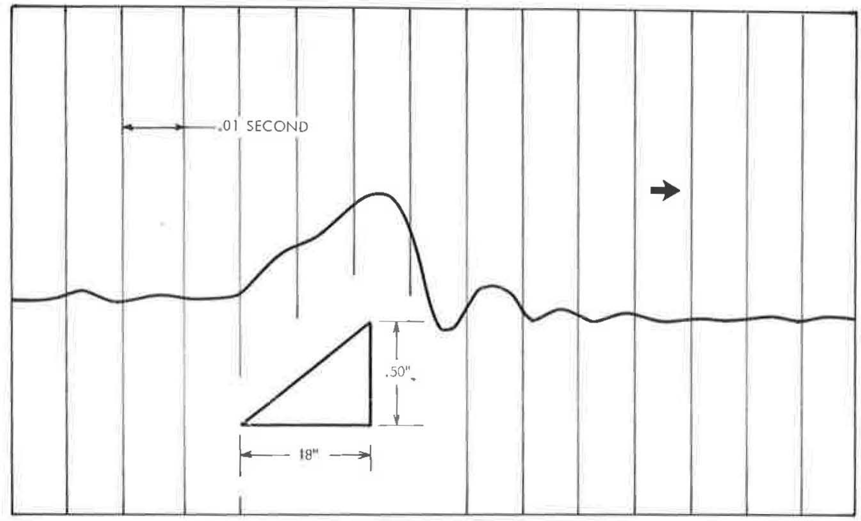

Figure 16. Transient response of road wheel passing over wood wedge at 40 mph.

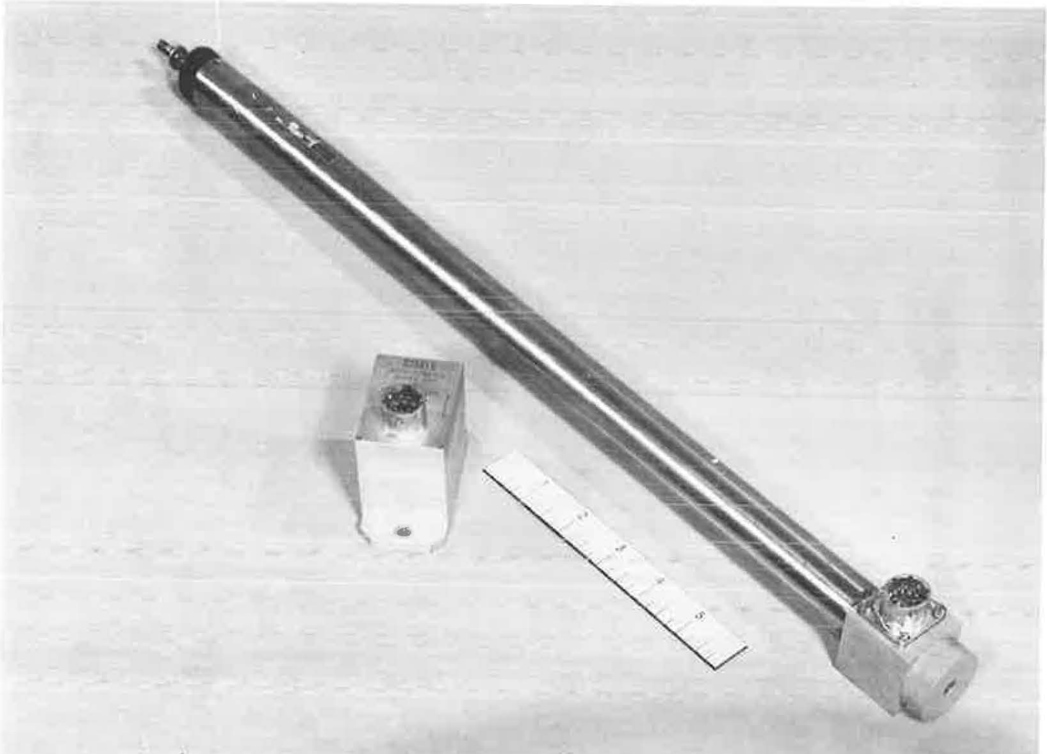

Figure 17. Systron-Donner accelerometer and Markite potentiometer.

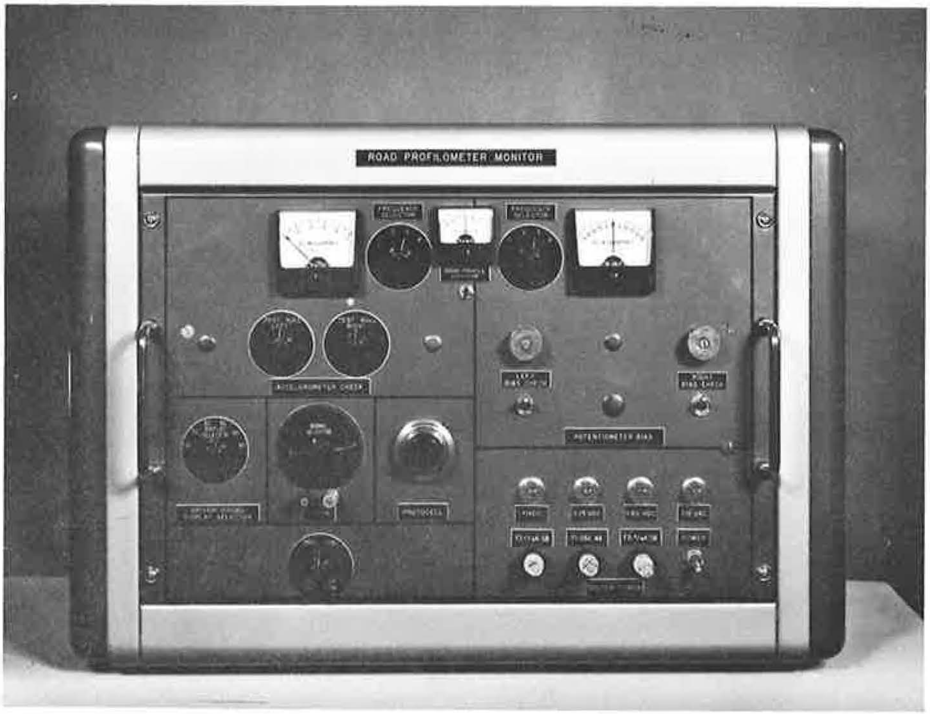

Figure 18. Monitor for road profilometer system.

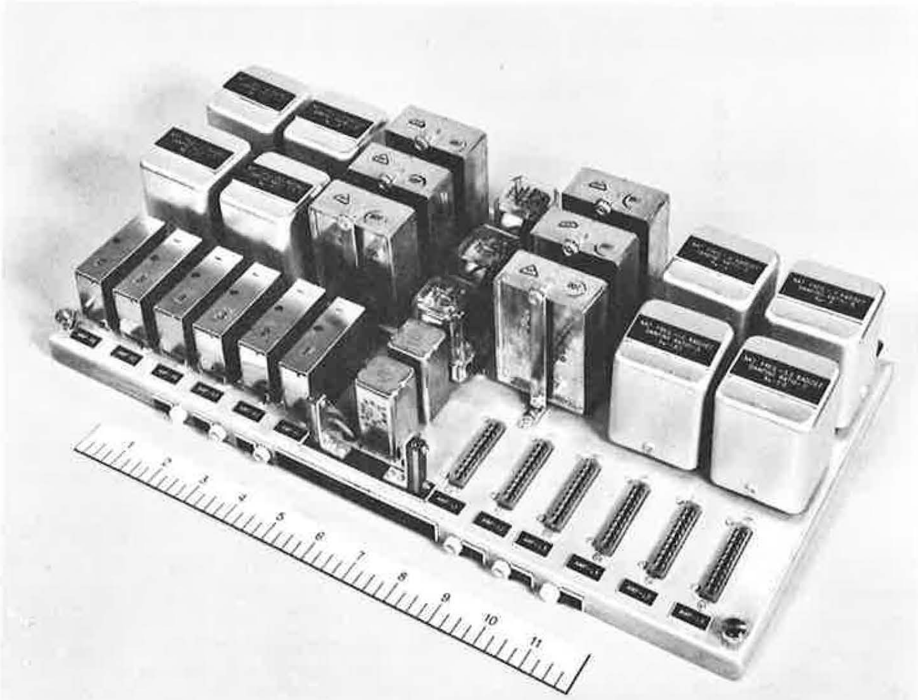

Figure 19. Analog computation package.

Transducers

Two important components in the road profile measuring system, the linear potentiometer and the accelerometer, are shown in Figure 17. The linear potentiometer is manufactured by the Markite Corporation. It has 15 in. of mechanical travel, 14 in. of electrical travel and is excited with a ±7-v DC power supply. This produces a road profile scaling of 1 in. of wheel displacement equal to 1 volt of output from the potentiometer.

The acceleration transducer is a Donner Model 4310 servo accelerometer. This is a force-balance instrument which has an improvement in linearity of 10 over conventional strain gage accelerometers. In addition, the accelerometer output signal is large enough that no signal amplification is required for use in the analog computation or for recording on a magnetic tape recorder. A ±2-g accelerometer range was found to be sufficient to handle the accelerations encountered at the mounting location on the vehicle body. The output signal for this range accelerometer is 3.75 v/g.

Precision excitation voltages must be supplied to both the potentiometer and accelerometer. A monitor box that performs this and several other functions is shown in Figure 18. The monitor box allows the operator to check quickly the condition of the transducers and to scale the signals for use in the analog computation or for recording on the tape recorder. A more complete description of the monitor box is given in Appendix B.

Analog Computation

The monitor box also contains a small, special-purpose analog computer (Fig. 19). A four-position selector switch (Fig. 20) mounted on the face of the monitor box allows the operator to select a variety of filter natural frequencies and voltage scaling. Corresponding to the positions on the selector switch are plug-in components inside the monitor box (Fig. 21) that actually establish the filter natural frequency and voltage scaling. Figure 22 shows the frequency response curve for 4 possible filter plug-in components. The filter natural frequency ω_f, the filter damping ratio ζ_f, and the voltage scaling in volts per inch of road profile K_w are indicated for each selection. A description of the analog computing components is given in Appendix B.

RECORDING EQUIPMENT

A large variety of equipment is available for recording road profiles as they are measured and computed. A direct-writing oscillograph is very valuable for an on-the-spot look at the road profile just measured. But it does not lend itself to more extensive data processing. For this purpose, a magnetic tape recorder is essential.

SYSTEM TRANSIENT RESPONSE

In addition to frequency response curves, information about the system performance can be obtained from the response of the system as a function of time, or transient response. Figure 23 shows the system transient response to a step input of displacement at the wheel which would occur if the road abruptly increased a unit in elevation. From a frequency standpoint, a step input is composed of all frequencies. The step is measured exactly at time equals zero indicating that the short wavelengths are almost unaffected by the filter. As time increases, the displacement returns to zero as the filter acts on the longer waves.

Figure 24 shows the transient response of the system to a ramp input such as would occur if the road abruptly increased in elevation at a rate of 1 unit per sec. This would simulate the transition from a level road to an uphill grade. The initial transition is measured exactly but, as time increases, the displacement again returns to zero. It now becomes obvious that this filtering action is necessary from a displacement storage standpoint; it is impossible to scale the problem to measure accurately both the small amplitude road features and the large amplitude hills.

The transient response to one wave of a sinusoid bump D ft long with flat road before and after the bump is shown in Figure 25. This transient response is for 40-mph

ROAD PROFILOMETER MONITOR

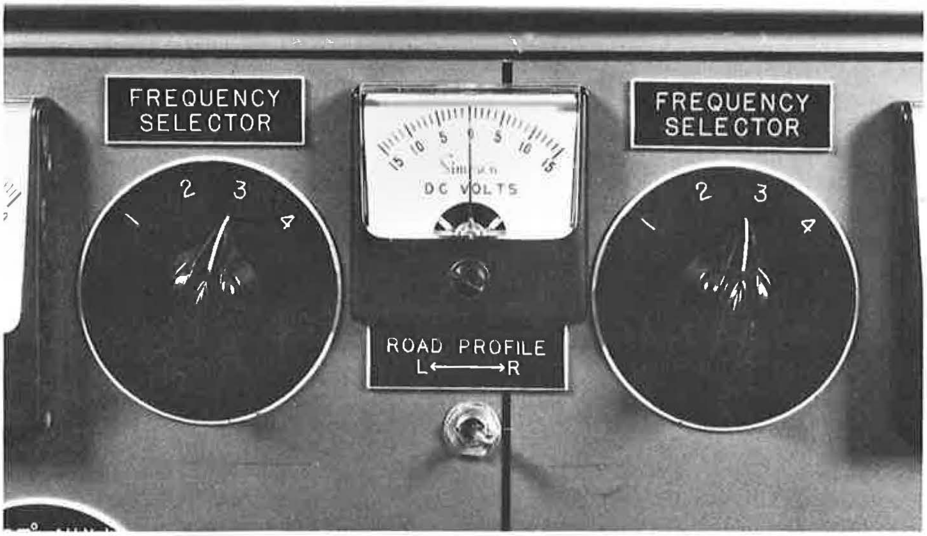

Figure 20. Frequency selector switch.

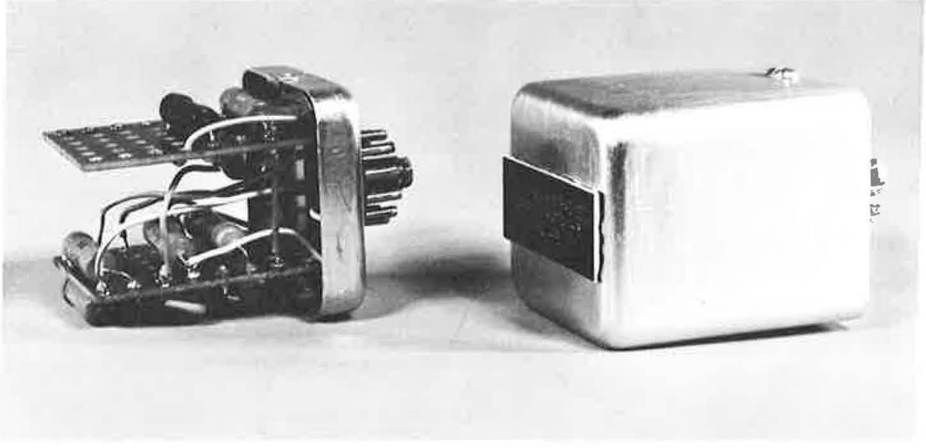

Figure 21. Frequency determining components.

recording velocity, a filter natural frequency of 0.3 rad/sec and a damping ratio of 0.5 for various values of D. As would be expected, the shorter bumps are measured with greater fidelity. Each bump is attenuated as the result of the filtering action on the longer wave components present in the bump.

The transient responses of Figure 25 can be determined for arbitrary values of recording vehicle speed, filter frequency and bump length as in Figure 26. Greatest fidelity is obtained when the quantity $(\omega_f D/V)$ is small. Again, the conclusion is that the long wavelength bumps are best measured with a high recording vehicle speed and low filter frequency.

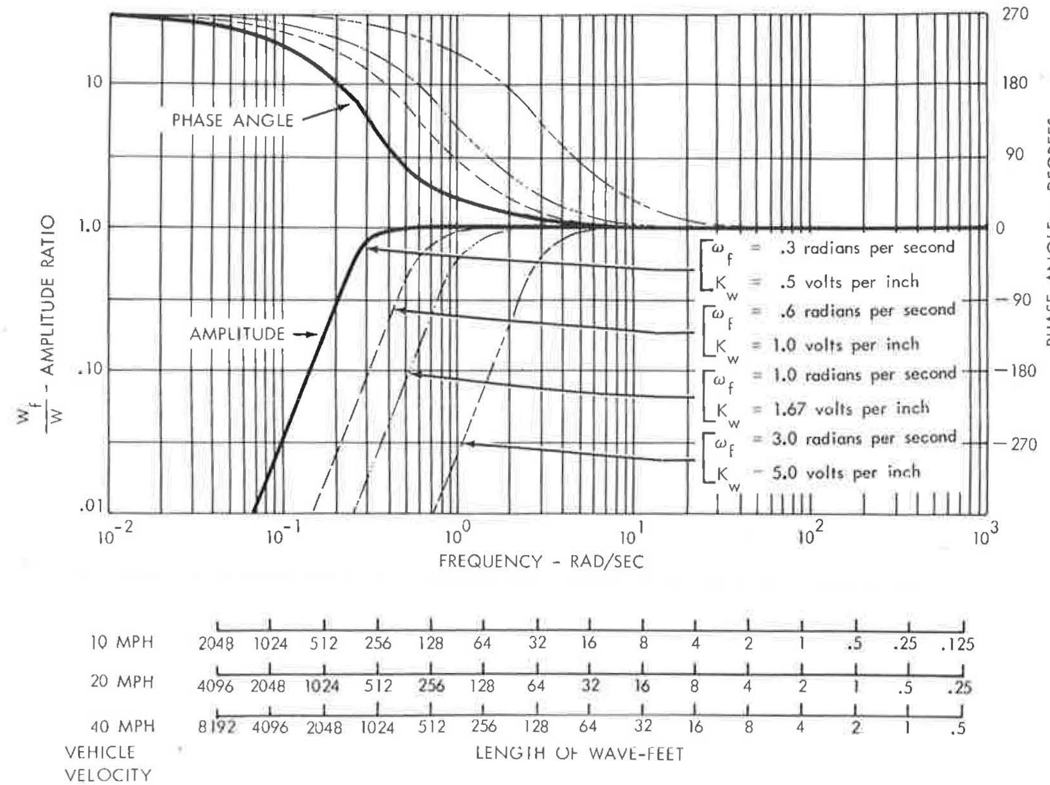

Figure 22. Typical frequency response selections.

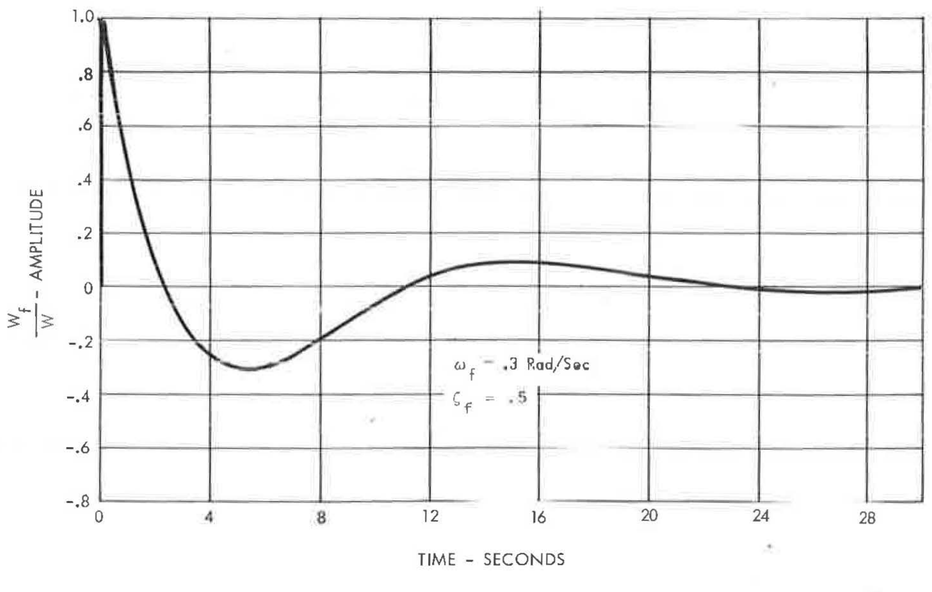

Figure 23. Transient response to a unit step input.

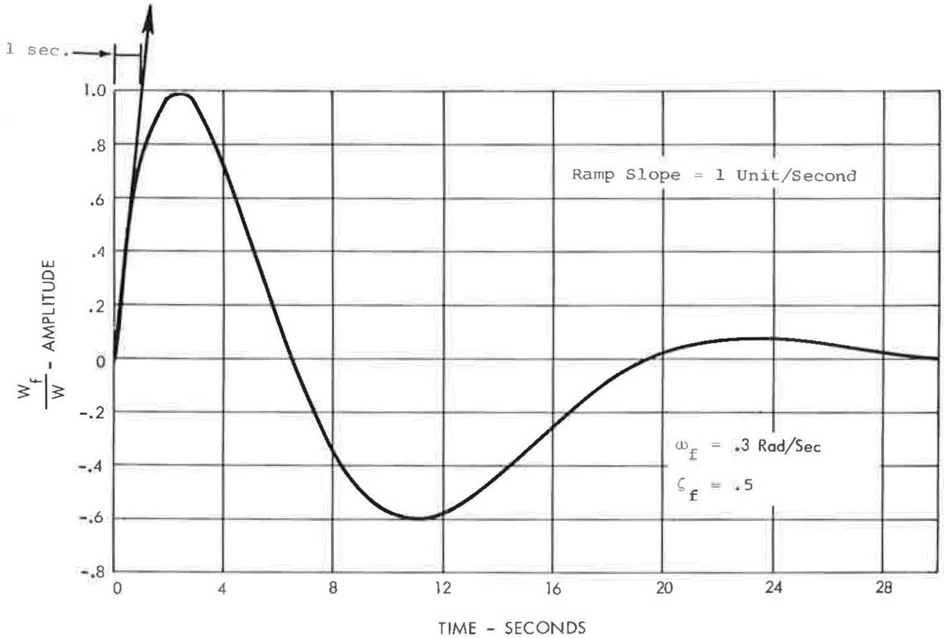

Figure 24. Transient response to a ramp input.

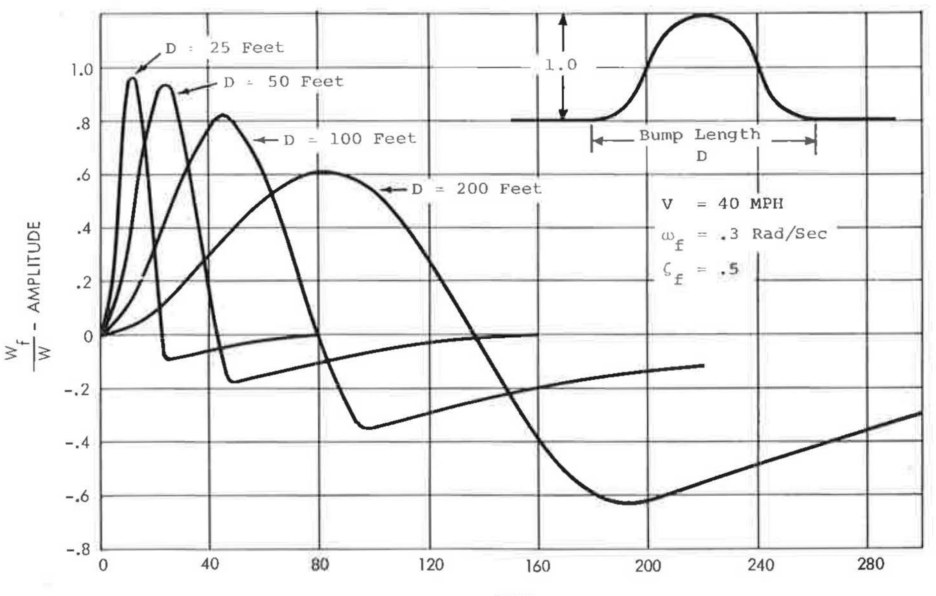

Figure 25. Transient response to a single sinusoid bump.

TYPICAL APPLICATION OF GMR PROFILOMETER

The GMR profilometer has been used on many projects, both within the General Motors Corporation and in cooperation with other groups. To illustrate the versatility

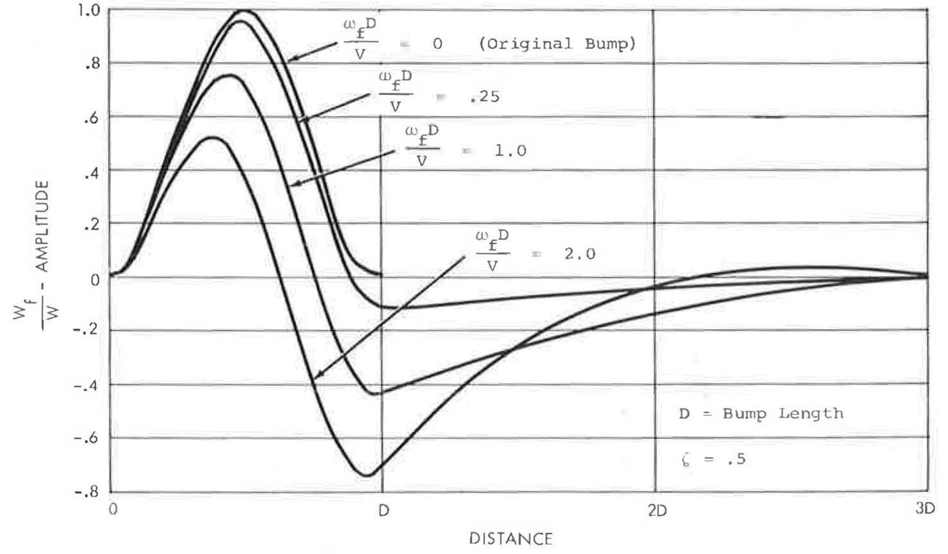

Figure 26. Measuring fidelity for a single sinusoid bump.

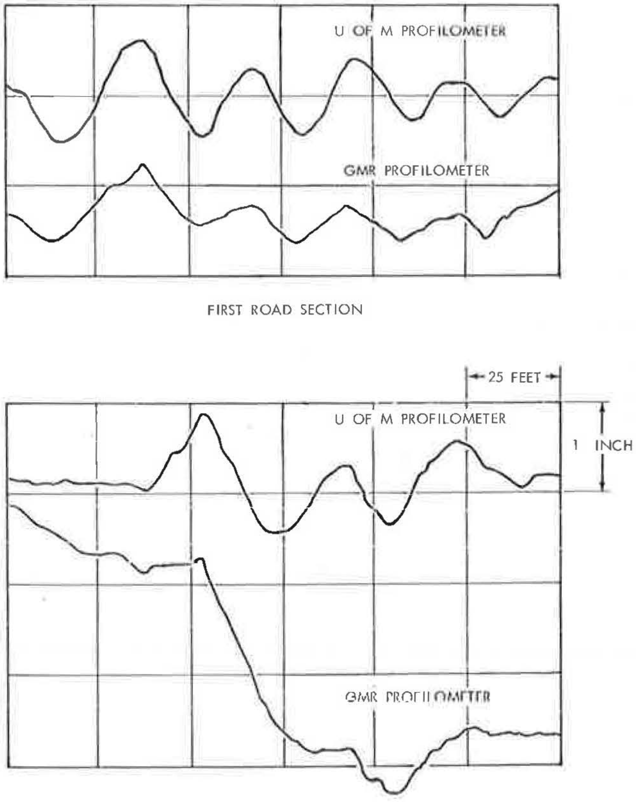

Figure 27. Comparison of profiles obtained with University of Michigan truck profilometer and GMR profilometer.

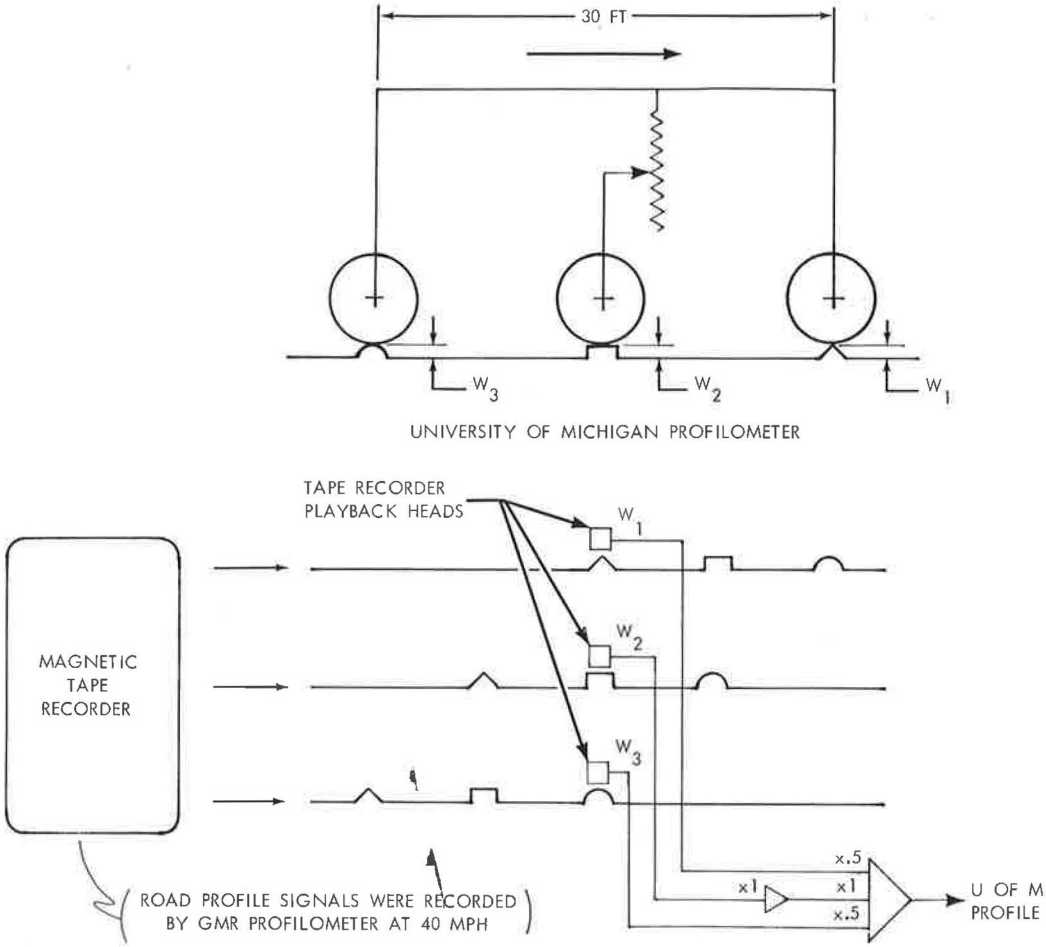

Figure 28. Simulation of rolling straightedge.

of the GMR profilometer, 3 applications are discussed showing how the profilometer was used and how the profiles were processed to produce meaningful test results.

Simulation of Moving Straightedge

In the first application the road profiles obtained with the GMR profilometer were compared with profiles obtained with the University of Michigan truck profilometer. This comparison consisted of measuring the same section of road with the 2 devices at the same time. Figure 27 compares profiles as obtained directly with the GMR profilometer and the University of Michigan truck profilometer for 2 sections of road. The comparison of the first section is surprisingly good and can readily be identified as the same road. The agreement of the 2 directly measured profiles for the second section is poor.

Better agreement is obtained in this comparison if a simulation is made of the University of Michigan profilometer being driven over the GMR measured road profile for the same section of road. The Michigan profilometer measures the difference between the height of its center wheel and the average height of its front and rear wheels. The simulation was implemented by using a magnetic tape recorder and several operational amplifiers (Fig. 28). The GMR road profile was recorded on the first track as it was measured. It was then played back from the first track onto the second track with a

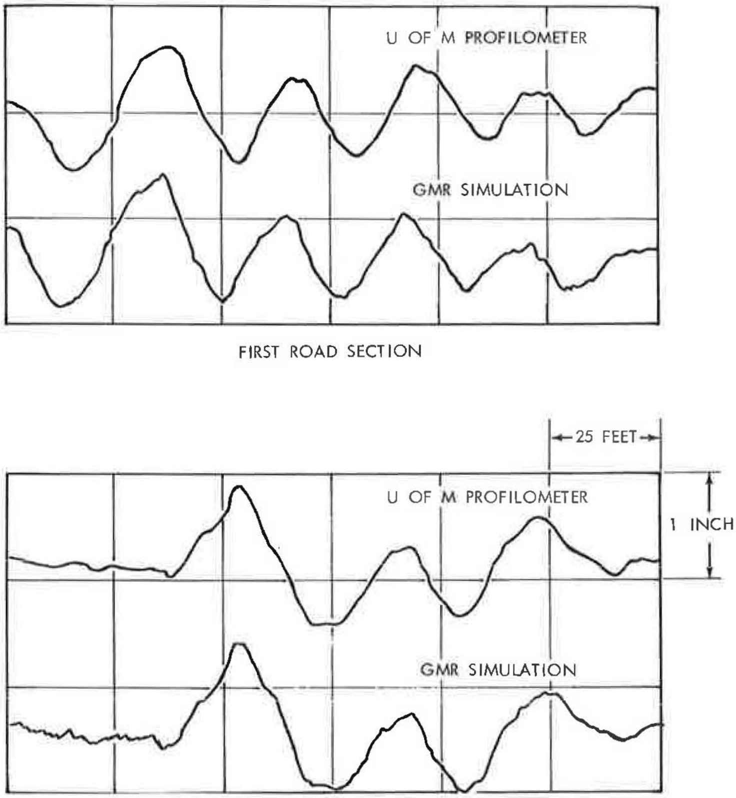

Figure 29. Simulation of University of Michigan profilometer.

time delay proportional to the distance between the first and second wheels of the moving straightedge. The third track was produced in a similar manner from the second track. The end result from this recording procedure is the availability of 3 signals that represent what each of the 3 wheels sees at any one time. The simulation is completed by the use of operational amplifiers to form

$$\text{U of M Profile} = W_2 - \frac{W_1 + W_3}{2}$$

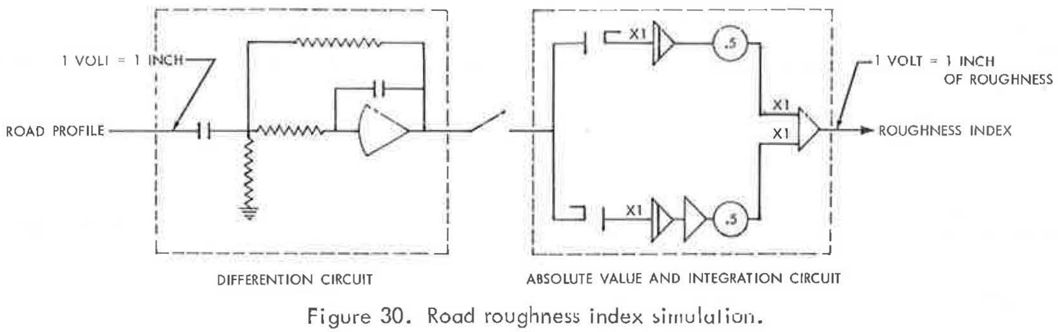

Figure 30. Road roughness index simulation.

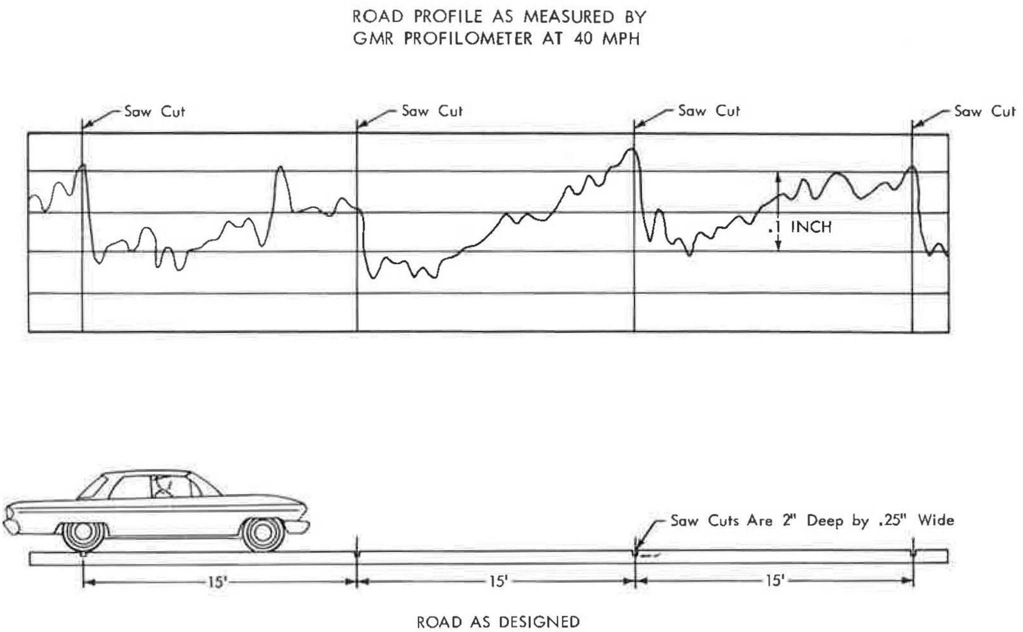

Figure 31. A road that induces automobile body shake.

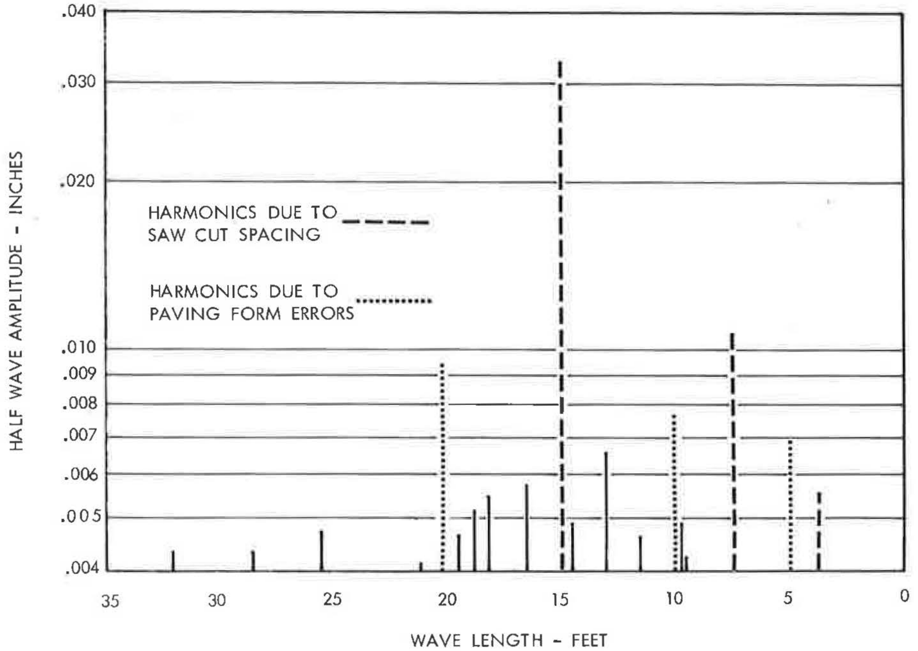

Figure 32. Harmonic analysis of a road that causes automobile body shake.

The comparison of the simulated moving straightedge profile with the actual moving straightedge profile as obtained with the Michigan profilometer is shown in Figure 29 for the 2 sections of road previously considered. The comparison is almost exact. This profilometer tends to amplify 30-ft wavelength components in the road profile

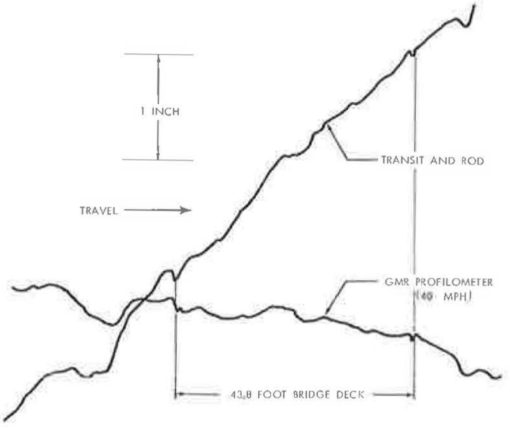

Figure 33. Bridge deck profiles as measured.

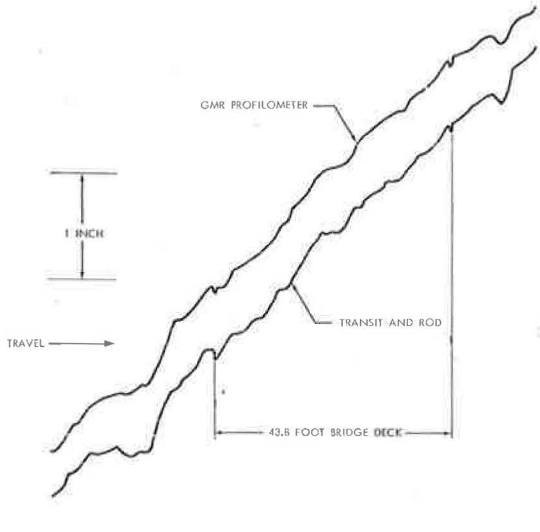

Figure 34. Comparison of bridge deck profiles after conversion of GMR profilometer reference.

(Figs. 27 and 29). The comparison in Figure 29 clearly indicates that the long wavelength components of the road profile, which are rejected by the GMR profilometer, are also rejected by the Michigan profilometer.

It is also possible to extend the simulation of the moving straightedge to obtain a roughness index (Fig. 30). Since the roughness index is an integration of vertical road displacement per unit distance, it can be obtained by differentiating the profile signal, integrating the plus and minus signals separately, dividing these signals by 2 and adding them together. Roughness indexes obtained by this simulation compared favorably with roughness indexes measured by the University of Michigan truck profilometer. In similar ways, other profilometers and roughness indexes can be simulated from the measured road profile.

Roughness indexes, of which currently there are several, are dependent only on the road profile and the method of measurement. Clearly, all the information about a road profile can only be obtained from its actual profile. Any of the roughness indexes currently available from other apparatus can be obtained from the measured GMR profile by simulation of the method of measurement.

More work is required to determine an index, or indexes, which will highly correlate with subjective ride observations. Any new index can be determined from the measured road profile.

Analysis of a Road Profile

The second application is more typical of the projects on which the GMR profilometer is used within General Motors Corporation. Figure 31 is a very much expanded profile of a road measured with the GMR profilometer. This road was laid continuously and then saw cut every 15 ft to provide weakened planes for cracking. The profile of this road appears to indicate that faulting has occurred at the saw cuts causing as much as $\frac{1}{8}$-in. discrepancy between adjacent slab heights. It is very difficult to assess mentally the seriousness of a wave form of this type on automobile ride. We do know from experience that this particular periodic wave form induces automobile body shake. Figure 32 illustrates one method used by Research Laboratories for analyzing a complex wave form to break it down into its frequency components or wavelength components. From this harmonic analysis (2), it becomes apparent that there is a rather large 15-ft component from the saw cut spacing with smaller second and third harmonics at 7.5-ft and 3.75-ft wavelengths. It was the 7.5-ft component near the speed limit of 60 mph that caused the body shake frequency of 11 cps. The harmonic analysis of Figure 32 gives us some additional information about this road. The next most prominent frequencies are

20-ft, 10-ft, and 5-ft wavelengths. The 20-ft wavelength is a form-laying-induced profile as shown below:

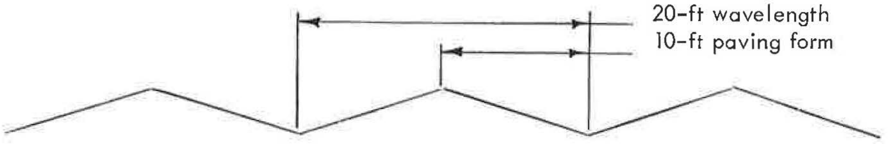

The 10-ft and 5-ft wavelengths are the second and third harmonics of the 20-ft wave. The 10-ft wavelength at 75 mph causes the same 11-cps body shake frequency.

Measurement of a Bridge Deck

The third application illustrates the use of the GMR profilometer to measure the profile of an interstate highway bridge deck. This bridge deck was measured by the Michigan State Highway Department as part of a Bureau of Public Roads research project to evaluate the GMR profilometer for highway department use. In this evaluation the profile of a bridge deck as measured with the Michigan State Highway Department's GMR profilometer was compared to the profile of the bridge deck as obtained with a transit and rod. The bridge deck profile measured by the 2 methods is shown in Figure 33. At first glance, it would appear that the comparison is poor, but a more detailed examination, keeping in mind the method of measurement, will show an excellent correlation. The most obvious discrepancy between the profiles is that the actual bridge rises approximately 2 in. in its length while the profile as measured with the GMR profilometer shows that it is dropping. This is due to the use of 2 different reference systems—a horizontal line for the transit and rod and a moving reference which is a function of the previous road profile for the GMR profilometer. The reason for this was discussed in the section on system transient response. Since the GMR road profile is always a function of the previous road profile, the GMR road profile will rarely show the correct slope.

A more direct comparison of the 2 profiles can be obtained by converting the reference of the GMR profile to a horizontal reference by the process in Appendix C, which requires knowing the actual elevation of 2 points along the road. Figure 34 compares the 2 profiles using the same horizontal reference system. In both profiles, there are small discontinuities where the bridge deck meets the road. There are also prominent profile characteristics that identify the profiles as being from the same road. The amplitude of local profile details is small, which demonstrates the resolution of the GMR profilometer. Since this bridge deck is relatively smooth and causes little disturbance as a car passes over it, the GMR profilometer appears to have more than adequate resolution for bridge deck measuring purposes.

The process of converting the reference system (Appendix C) is another example of data processing at a later time to put the original information into more meaningful form. Whether this form be road profile, roughness index, moving straightedge profile, slope variance, harmonic analysis, power spectral density, or any other, it is felt that this final form can be obtained from the GMR profilometer data. The authors are not proposing that any of the data processing methods discussed be adopted by the highway industry, but rather are indicating the wide variety of information which can be obtained from the measured road profile with later data processing techniques.

CONCLUSIONS

1. The GMR road profilometer developed by the General Motors Research Laboratories is simple to operate and produces an accurate and repeatable road profile quickly and safely.
2. The measured road profile when recorded on magnetic tape can be reproduced easily for data processing at a later date.

3. The road profile and roughness index as measured by the University of Michigan profilometer can be obtained from the profile measured with the GMR road profilometer.
4. All of the roughness indexes currently in use can be obtained from the profile measured with the GMR road profilometer.
5. The operating characteristics of the GMR road profilometer are variable and can be changed to adapt to the conditions of the road being measured.
6. Additional work is required to determine a roughness index, or indexes, which will correlate highly with subjective ride observations. These various indexes can be determined from the profile measured with the GMR road profilometer.

REFERENCES

1. Spangler, E. B., and Kelly, W. J. Servo-Seismic Method of Measuring Road Profile. Highway Research Board Bull. 328, pp. 33-51, 1962.
2. Wylie, C. R. Advanced Engineering Mathematics. McGraw-Hill, New York, 1960.
3. Chestnut, H., and Mayer, R. Servomechanisms and Regulating System Design. John Wiley and Sons, New York, 1959.

Appendix A

FREQUENCY RESPONSE THEORY

Analysis by the frequency response (3) approach is based on the fact that any complex wave form can be represented by the summation of several sinusoidal waves. For example, the wave form at the top of Figure 35 can be manufactured by the algebraic summation of 2 sinusoidal waves as shown at the bottom of the figure. The first sinusoid wave is called the fundamental or first harmonic. The length of the second wave is one-half the first wave and is called the second harmonic. At time equals zero, both sinusoid waves are passing through zero amplitude going in the same direction (upward); thus there is no phase shift between these 2 sinusoid waves in this complex wave form. To illustrate the effect of phase shift, Figure 36 shows the same 2 sinusoidal waves with the fundamental only shifted 45°. The resulting wave form is, of course, also modified. In the frequency response approach it is then assumed that a system can be analyzed by observing how the system responds to the individual sinusoidal waves that make up the complex wave form.

A simple method of performing a frequency response measurement on a system

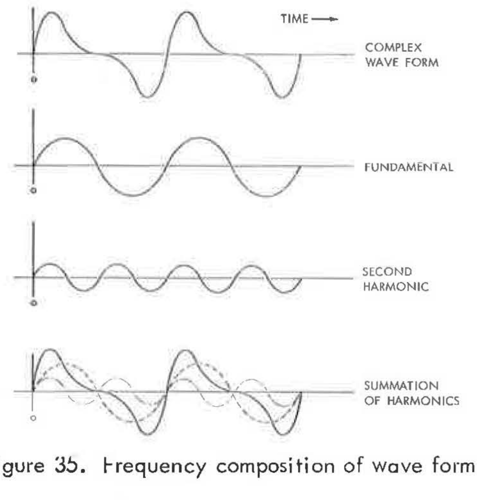

Figure 35. Frequency composition of wave form.

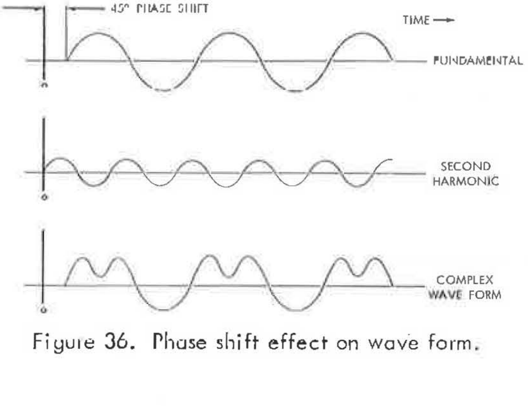

Figure 36. Phase shift effect on wave form.

is to use a sinusoidal signal as an input to the system and observe its output. The output from this test is usually presented as amplitude ratio and phase shift. The amplitude ratio is the amplitude of the output signal divided by the amplitude of the input signal. The phase shift can also be determined by observing how much the output signal leads or lags the input signal. As an example, the frequency response of the GMR profilometer system (Fig. 11) could have been obtained by driving the truck over many different sinusoidal wave roads and recording amplitude ratio and phase shift for each wave. This is not practical because these sinusoid roads do not exist, and it is not necessary because the frequency response of this system can be computed.

Appendix B

GMR ROAD PROFILOMETER MONITOR

Analog Computation

In the early GM profilometer, the analog computation was performed in a rather large general purpose analog computer carried in the measuring vehicle. However, once the analog computer requirements were more specifically determined, a special analog computation package was designed to fit the job exactly. This analog computation package (Fig. 19) is mounted on a separate sub-chassis in the monitor box. The main analog computing components are small solid-state operational amplifiers manufactured by Philbrick Research Incorporated. The operational amplifiers are converted to an integrator by the addition of a good quality capacitor between the output and input of the amplifier. The operational amplifiers form a network that performs the functions of double integration, signal summation and high pass filtering. The analog computation package has 4 plug-in frequency determining components which can be individually selected by the switch (Fig. 20). The operator can select the filter natural frequency and voltage scaling used in the analog computation. A simple test has been built into the analog computation system to check the condition of the analog components. The test is performed by rotating the calibration switch on the face of the monitor box. The calibration switch replaces the output from the linear potentiometer, $(W-Z)_m$, with a 1-v signal. Since the potentiometer is scaled to 1 v = 1 in. of road profile, the 1-v calibration signal will always represent a 1-in. step of displacement. The output W_f should resemble the step transient response of Figure 23. The time for the transient response to first cross the zero axis and the amount of overshoot are good checks on the operation of the circuit. The overshoot for a 0.5 damping ratio will always be approximately three tenths of the step value. The time in seconds required for the transient response to first cross the zero axis can be expressed as a function of the filter natural frequency in radians per sec by

$$t = \frac{0.74}{\omega_f}$$

From Figure 23, the time is 2.5 sec as predicted by this equation.

Other Monitor Functions

Although the basic system of the GMR road profilometer is simple, the associated functions necessary to make everything work become a bit complex. It is desirable to reduce this complexity to the point where it is reliable and can be operated by a person with limited technical background. Other than analog computation, the purpose of the monitor is to:

1. Convert 110-v 60 cycle AC power into suitable DC power supplies for transducer excitation;
2. Supply checks to determine if all power supplies are working;
3. Check on the operation of all transducers;
4. Receive all transducer signals and convert them into signals suitable for analog computation to produce road profile; and
5. Supply properly scaled road profile signals for recording on a 1-v RMS range tape recorder.

The monitor has a power supply cable which can be plugged into any 110-v 60 cycle power supply. In a vehicle this may be the same converter used to supply power to an oscillograph or a tape recorder. The monitor has a power switch which interrupts the 110-v supply when it is in the OFF position; when the switch is ON, the 110-v alternating current is converted into ±60-v DC, ±15-v DC, and + 1-v DC. The monitor control panel (Fig. 18) is equipped with yellow indicator lights which light if there is an output from each of the DC voltage regulators. The indicator light only shows that the DC voltage regulators have an output. However, experience shows that if a regulator has any output, it almost always is the correct voltage. These DC voltages are necessary for successful operation. If a light is out, the reason should be determined before proceeding further.

In addition to supplying transducer excitation, the monitor unit supplies excitation for a photocell sensor. A light shines on the pavement from under the vehicle. A photocell aimed at the light spot senses changes in pavement reflectivity. With this device, areas of interest on the road can be marked with contrasting paint, which then produce signals as they are passed over. In addition to indicating painted areas, the photocell has been found to indicate tarred pavement joints, saw cuts and cracks. Preliminary results indicate that this device could be used by highway people in pavement condition checks.

Connectors have been supplied on the back of the monitor (Fig. 37) for all the transducer cables. After connecting the transducers, the condition of each transducer can be evaluated by a few simple checks. In the ACCELEROMETER CHECK area of the

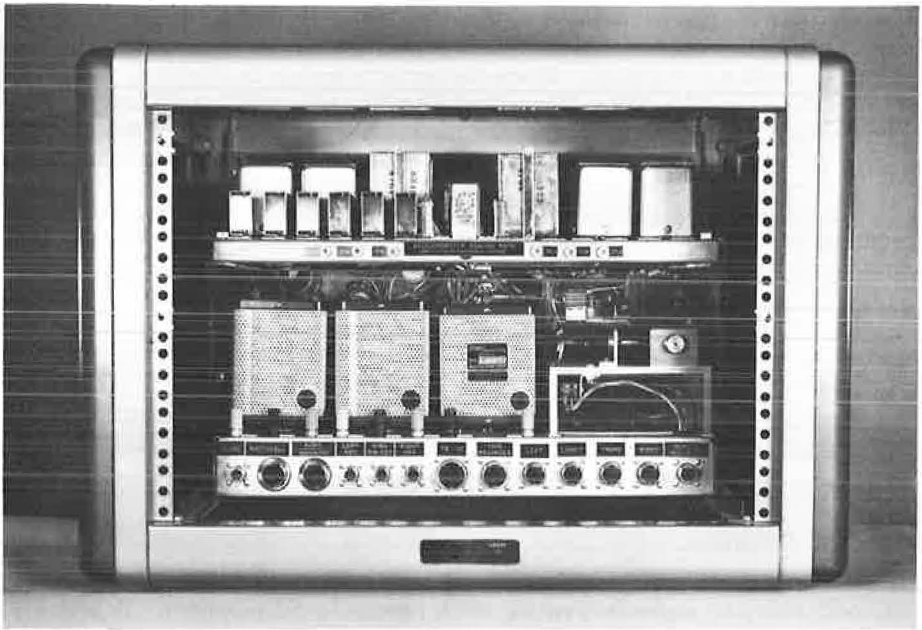

Figure 37. Transducer connectors on rear of monitor box.

monitor control panel (Fig. 18) is a rotary switch for the accelerometer check. Turning the switch counterclockwise to TEST should deflect the meter 1 milliampere which indicates that a test is being performed. Turning the switch clockwise to NULL should cause no meter deflection. Readings different from these indicate the accelerometer is not functioning properly. The rotary switch is spring loaded to return to the normal operating position.

In the POTENTIOMETER BIAS area of the monitor control panel is a biasing pot for the potentiometer. A potentiometer output results from the brush of the potentiometer being located at a non-zero voltage spot on the element. The voltage output of the potentiometer can be observed on the meter by pressing down the toggle switch and the output can be made zero by adjusting the biasing pot with a screwdriver. It is desirable to have the potentiometer output nearly zero prior to recording so that the signal fluctuates around zero. The output of the potentiometer changes as the vehicle load changes since this changes the linear potentiometer arm position.

The remaining transducer inputs into the monitor box are a photocell output and a rotating cable from the measuring vehicle's transmission output speed. To supply the rotating flexible cable to the monitor box it is necessary to install a tee on the transmission where the vehicle's speedometer cable is attached. The flexible cable from the transmission has a receptacle on the monitor box into which it fits during operation. Inside the monitor box, the rotating cable drives a tachometer generator and a distance measuring device.

In the center of the monitor control panel is an adjustable potentiometer labeled PHOTOCELL. This is an adjustment on the photocell voltage output for various road reflecting conditions.

To the left of the monitor control panel is an area labeled DRIVER VISUAL DISPLAY SELECTOR. This selector switch is used in conjunction with a driver display box (Fig. 38) located in front of the driver on the vehicle's instrument panel. The driver display box is connected by electrical cables and connectors to the monitor box. There are 2 meters on the driver display box. One meter, labeled SPEED, will read zero when the driver is driving at the speed selected on the monitor panel. This meter is in effect a more sensitive speedometer. In Figure 18, the selector switch is set at 40 mph. Other speeds are available from 10 mph to 60 mph in steps of 10 mph. The second meter on the driver display box, labeled INFORMATION, is a monitor of the information signal. The information signal display is the output of a tachometer-generator which is vehicle velocity. Distance is indicated by a reversal in sign of the voltage every tenth mile traveled. The voltage level can be reduced to zero

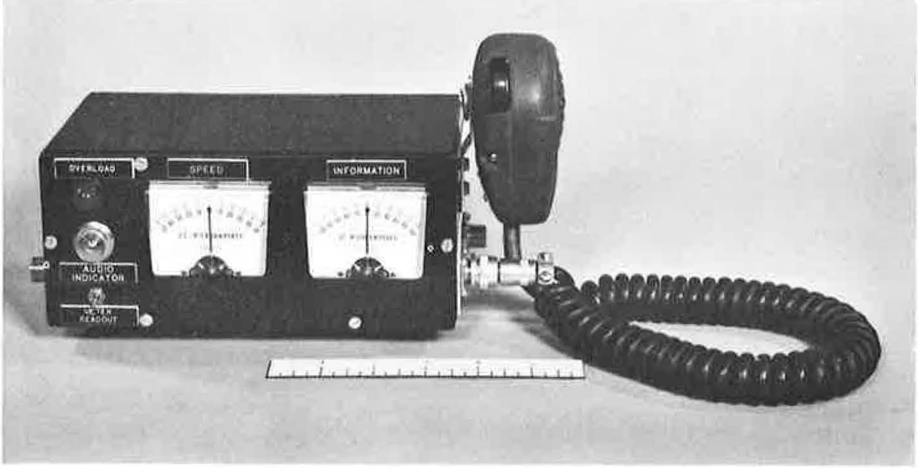

Figure 38. Driver display box.

with a driver-operated remote switch to mark events of interest. A typical output of this device is:

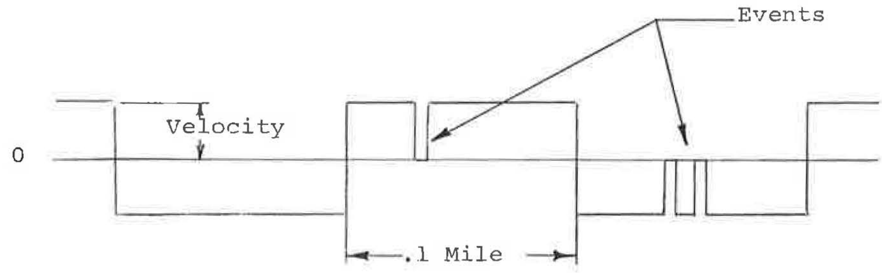

The driver also has available a microphone with which he is able to record voice comments on the tape recorder. As an indication that the voice signal has been supplied to the tape recorder, an AUDIO INDICATOR in the form of a light bulb is mounted on the driver display box. This bulb glows as signal amplitude increases.

The monitor box has 3 outputs. One output is a connector to a tape recorder or oscillograph. The signals to the recorder are scaled not to exceed 1 volt RMS. A second connector contains the outputs from the transducer for use in an external analog computer. A third output is a SCOPE connection and a SIGNAL SELECTOR switch which allows the signals going to the tape recorder to be observed on an oscilloscope.

Appendix C

REFERENCE SYSTEM CONVERSION

Because there is no direct relationship between the slope of the road profile from the GMR profilometer and the actual slope of the road, it is sometimes difficult to compare the GMR road profile with the real road. This comparison can be simplified by converting the reference on the GMR profile to a horizontal reference. Figure 39 establishes the geometry to be used in the development of the conversion process.

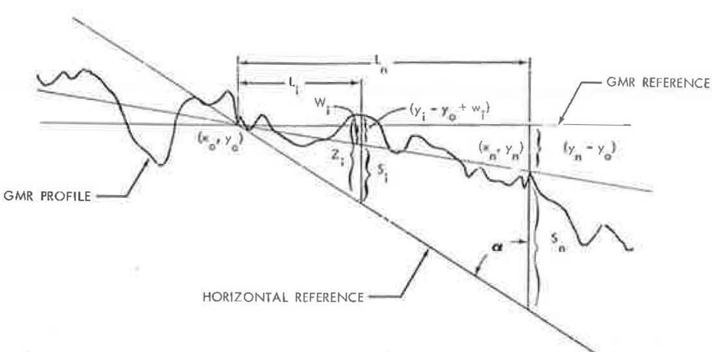

Figure 39. Reference conversion geometry.

The following notation is used in this appendix:

(x_i, y_i) = the location of a point on the GMR profile, the elevation of which is to be determined;
(x_o, y_o) = the location of the first point on the GMR profile at a known elevation;
(x_n, y_n) = the location of a second point on the GMR profile at a known elevation;
S_n = difference in elevation between two points (x_o, y_o) and (x_n, y_n) on the road surface as measured by a transit;
L_n = horizontal distance between two points (x_o, y_o) and (x_n, y_n) of known elevation;
Z_i = elevation of a point on the road profile; and
L_i = horizontal distance from point (x_o, y_o) to point (x_i, y_i).

Figure 39 is greatly compressed in the horizontal direction and makes the angle α appear much smaller than 90°. Actually, it is very near 90° and will be considered 90° for this analysis.

By observation the following relationships can be written:

$$S_i = S_n \frac{(x_i - x_o)}{(x_n - x_o)}$$

$$W_i = (y_n - y_o) \frac{(x_i - x_o)}{(x_n - x_o)}$$

$$Z_i = (y_i - y_o + W_i + S_i)$$

$$L_i = x_i - x_o$$

This reference conversion can be performed in a variety of ways depending upon the frequency of its use. The simplest and slowest method is to measure the distances Z_i directly from the oscillographic recording (Fig. 39). A digital computer program could be used to obtain fast, but possibly complex, conversion of the reference. In the bridge deck problem the Michigan State Highway Department recorded the bridge profile on an oscillograph chart and the profile was digitized using a Benson-Lehner digitizer.

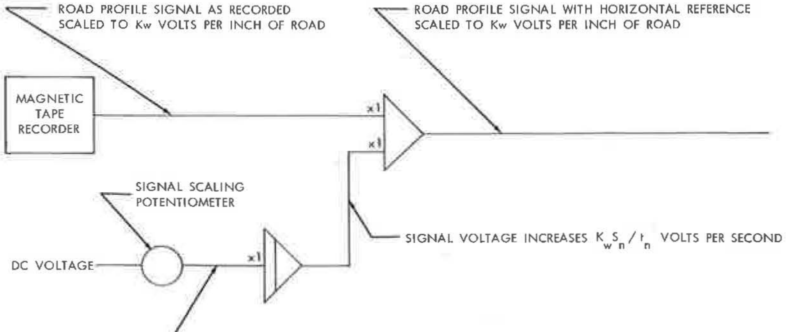

Figure 40. Analog reference conversion.

If the road profile is recorded on magnetic tape, this reference conversion can be accomplished on the analog signal as shown in Figure 40. S_n (Fig. 39) is the difference in elevation between 2 points on the road surface in inches as measured by a transit and t_n is the time in sec required by the magnetic tape recorder to play back the road distance L_n. K_w is the road profile scaling in volts per inch as it is played back from the tape recorder. If the analog signal is available, the analog method of reference conversion is the simplest.